



## Research paper

## Organoseleno cytostatic derivatives: Autophagic cell death with AMPK and JNK activation

Pablo Garnica<sup>a, b</sup>, Ignacio Encío<sup>b, c</sup>, Daniel Plano<sup>a, b</sup>, Juan A. Palop<sup>a, b</sup>, Carmen Sanmartín<sup>a, b, \*</sup><sup>a</sup> Universidad de Navarra, Facultad de Farmacia y Nutrición, Departamento de Tecnología y Química Farmacéuticas, Campus Universitario, 31080, Pamplona, Spain<sup>b</sup> Instituto de Investigación Sanitaria de Navarra (IdiSNA), Irunlarrea 3, E-31008, Pamplona, Spain<sup>c</sup> Department of Health Sciences, Public University of Navarra, Avda. Barañain s/n, E-31008, Pamplona, Spain

## ARTICLE INFO

## Article history:

Received 18 February 2019

Received in revised form

17 April 2019

Accepted 29 April 2019

Available online 4 May 2019

## Keywords:

Autophagy

Cancer

Cyclic imide

Diselenide

Selenocyanate

## ABSTRACT

Selenocyanates and diselenides are potential antitumor agents. Here we report two series of selenium derivatives related to selenocyanates and diselenides containing carboxylic, amide and imide moieties. These compounds were screened for their potency and selectivity against seven tumor cell lines and two non-malignant cell lines. Results showed that MCF-7 cells were especially sensitive to the treatment, with seven compounds presenting GI<sub>50</sub> values below 10 μM. Notably, the carboxylic selenocyanate **8b** and the cyclic imide **10a** also displayed high selectivity for tumor cells. Treatment of MCF-7 cells with these compounds resulted in cell cycle arrest at S phase, increased levels of pJNK and pAMPK and caspase independent cell death. Autophagy inhibitors wortmannin and chloroquine partially prevented **8b** and **10a** induced cell death. Consistent with autophagy, increased Beclin1 and LC3-IIB and reduced SQSTM1/p62 levels were detected. Our results point to **8b** and **10a** as autophagic cell death inducers.

Published by Elsevier Masson SAS.

## 1. Introduction

Despite recent advances in development of anticancer agents, this illness remains a leading cause of disease-related death worldwide [1]. Due to their effect on several survival or death signaling pathways that may decide the fate of cancer cells [2,3], therapies based on autophagy targeted agents are now in the focus of a wide range of researchers. Among the signaling pathways implicated in these processes, JNK activation has been proven to participate in multiple autophagic events such as Beclin1 expression and autophagic-mediated cell death [4,5]. Energetic stress has also been described to be a trigger for autophagy [6]; in this context, AMPK has been proven to have an essential role promoting autophagy by inhibiting the mTORs regulatory cascade [7]. The phosphorylation of AMPK and JNK in autophagy-mediated cell death has been previously described in breast adenocarcinoma [8,9] and several other cancer types such as myeloma [10] and leukemia [11].

During the past decade, extensive studies of selenium compounds have demonstrated their antitumor and chemopreventive activities in a vast array of experimental models [12]. These derivatives interfere with the redox homeostasis and signaling of cancer cells. The mechanism by which they cause their effect include alterations in cell cycle checkpoints, proliferation, senescence, and death pathways [13]. In addition, some selenium derivatives such as selenite, selenocysteine and Se-allylselenocysteine play an effective role in cancer treatment as autophagy inducers and modulators of the JNK signaling pathway [14–17].

Many chemical entities containing selenium, with potent anti-tumor activity, have been explored by the scientific community. Among them, selenocyanate [18] and diselenide [19] moieties have been highlighted due to their interesting antitumor properties. In this line of investigation two effective derivatives, the diselenide analog bis(4-aminophenyl)diselenide (**0a**) and the corresponding selenocyanate (**0b**), were recently identified in our laboratory [20]. In order to obtain a second generation of selenium structures with improved activity, selectivity and water solubility these compounds have been used as a starting point to continue with their modulation [21]. It is remarkable that one of the limitations of the selenium derivatives is their poor water solubility which is detrimental for

\* Corresponding author. Department of Pharmaceutical Technology and Chemistry, University of Navarra, Irunlarrea, 1, E-31008, Pamplona, Spain.

E-mail address: [sanmartin@unav.es](mailto:sanmartin@unav.es) (C. Sanmartín).

their bioavailability and drug development. To obtain compounds with improved pharmacokinetic properties, modifications in the hydrophobic scaffold that improve water solubility are usually assayed. As an example of this strategy, introduction of a hydroxyl group in the phenyl ring of the natural product camptothecin has been shown to counteract efficiently this drawback [22]. Thus, a useful option when using this approach is to incorporate polar functional groups, such as acidic or basic groups. These fragments enable the possibility of salt formation and therefore might enhance water solubility [23,24]. In this study, substantial efforts had been directed towards finding different chemical scaffolds that, while maintaining the cytotoxic activity, should increase the hydrophilicity further contributing to the solubility optimization. Among the structural features incorporated, we surmised that the introduction of the carboxylic core could be a logical approach for improving its aqueous solubility. This moiety is present in widely described organoselenium compounds such as 3,3'-diselenodipropionic acid [25]. In addition, the dicarboxylic acids are of special importance because of their versatility in the preparation of the corresponding cyclic imide homologs which are widely described in the literature as potential antitumor agents [26,27].

Taking into consideration the facts stated above and our previous work in the field of new selenium compounds as antitumor agents [21,28–33], the present study aimed to synthesize selenocyanates and diselenides containing carboxylic, amide and imide moieties. The general outline of this series of compounds is presented in Fig. 1. Variations were made in the group linked to the carboxy feature through selection of different cyclic symmetric anhydrides commercially available such as maleic, succinic, phthalic ... Finally, with the objective of widening the structural variations, a new anhydride was synthesized through the Diels-Alder cycloaddition. The rationality behind this proposal is the synthesis of a structural analog of norcantharidin, a well-known active antitumor autophagy inducer [34].

## 2. Results and discussion

### 2.1. Chemistry

The seventeen compounds synthesized and presented in this

work can be categorized into two different subseries according to their selenium moiety:

- Diselenide derivatives containing carboxylic and amide or imide moieties (**1a-3a**, **5a**, **7a-11a**).
- Selenocyanate derivatives containing carboxylic and amide moieties (**1b-8b**).

The resulting compounds were numbered according to the corresponding anhydride used as starting material.

Derivatives were synthesized following the synthetic path depicted in Fig. 2. The corresponding anhydrides were reacted with either bis(4-aminophenyl)diselenide (**0a**) or 4-aminophenylselenocyanate (**0b**) in acetone at room temperature for 8 h up to 24 h. The formed precipitate was filtered and washed with *n*-hexane or ethyl ether to yield the final compounds. The mechanism proposed for this reaction is a nucleophilic acyl substitution illustrated in Fig. 3A. Moreover, all our attempts to generate derivatives **4a** and **6a** were unsuccessful since the reaction of the corresponding anhydrides with **0a** in different conditions (temperature, solvents and catalyst) failed to yield the desired compound. Unfortunately, the alternative strategy of reducing their selenocyanate analogs (**4b** and **6b**) to obtain derivatives **4a** and **6a** under different conditions only resulted in the degradation of the start-up derivatives. To obtain the cyclic imides (**9a-11a**), the corresponding amidic acids (**1a**, **2a**, **5a**) were heated in presence of acetic anhydride and sodium acetate. This reaction probably starts by a deprotonation of the carboxylic group, followed by the nucleophilic attack of the oxygen to the carbonyl group on the acetic anhydride followed by a subsequent intramolecular cyclization to yield the final cyclic imides. The reaction was quenched with water causing the prompt precipitation of the desired compound. The proposed mechanism of reaction to yield the cyclic imides is exemplified in Fig. 3B.

### 2.2. Biology

#### 2.2.1. Cytotoxicity and antiproliferative activity

The cytotoxic potential of the seventeen synthesized compounds was evaluated against a panel of cell lines including seven

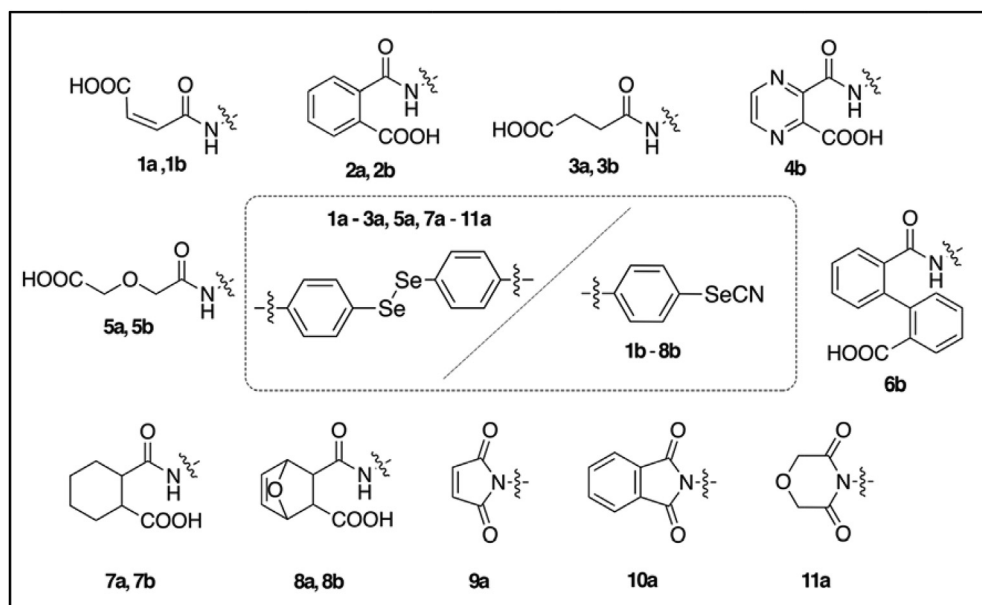


Fig. 1. Structures of novel selenium containing compounds.

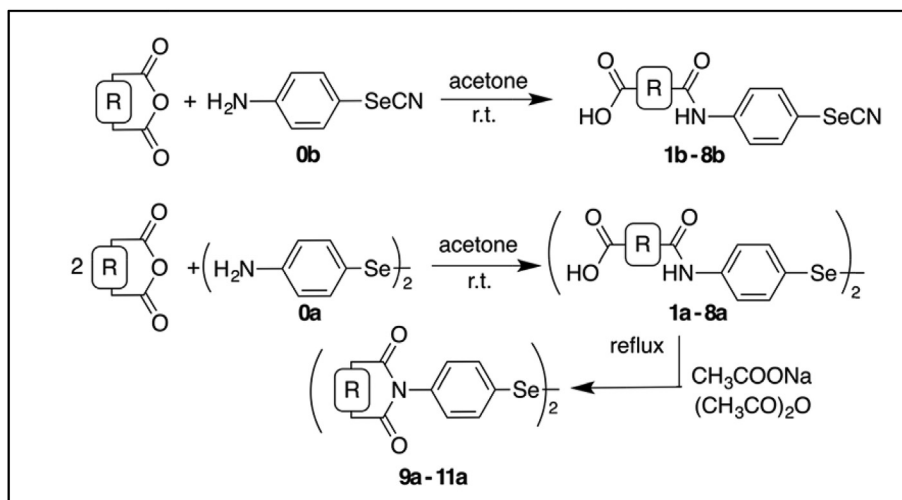
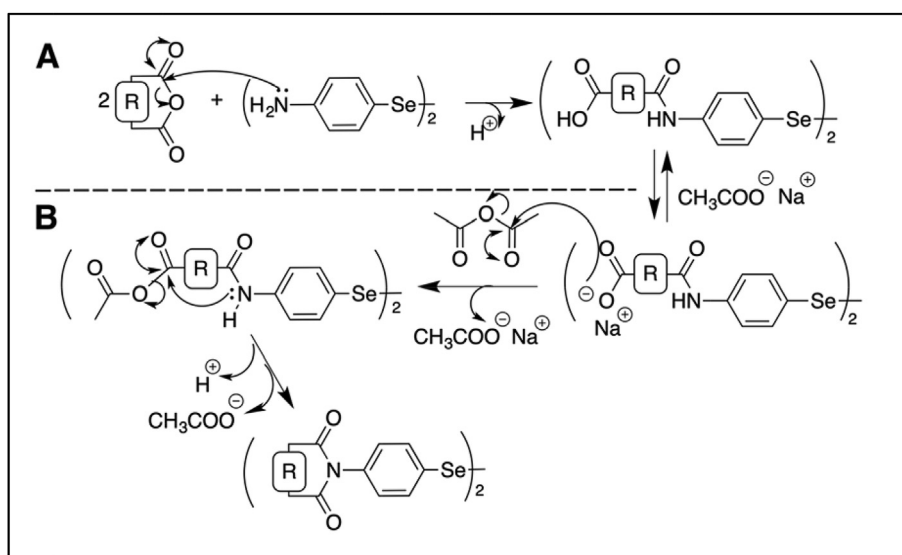


Fig. 2. General procedure of synthesis.

Fig. 3. Mechanism proposed for the synthesis diselenide derivatives. Mechanism proposed for the synthesis of compounds **1a-3a**, **5a** and **7a-8a** (A). Mechanism proposed for the synthesis of cyclic imide derivatives **9a-11a** (B).

different cancer cell lines and two other cell lines derived from non-malignant tissue. Evaluation was performed at 48 h treatment following the MTT (3-(4,5-dimethylthiazol-2-yl)-2,5-diphenyltetrazolium bromide) methodology as previously described [33]. The cancer cell lines included in the panel were PC-3 (prostatic adenocarcinoma); HTB-54 (lung carcinoma), and HT-29 (colon carcinoma); MOLT-4 and CCRF-CEM (acute lymphoblastic leukemia); K-562 (chronic myelogenous leukemia) and MCF-7 (breast adenocarcinoma). The selected cell lines derived from non-malignant tissue were 184B5 and BEAS-2B. Cisplatin was used as positive control. In addition, the parent compounds bis(4-aminophenyl)diselenide (**0a**) and 4-aminophenylselenocyanate (**0b**) were tested as a reference to identify whether the second generation compounds accomplished the objective of improving potency and selectivity.

To narrow down the number of derivatives moving on to the full dose-response cytotoxic profiling assay, a two-dose concentration (100  $\mu$ M and 10  $\mu$ M) screening was first performed. The results obtained for the 10  $\mu$ M treatment are shown in Fig. 4. As shown in

the figure, MCF-7 cells were the most sensitive cells toward the tested derivatives. In fact, seven compounds (**1b**, **2b**, **4b**, **8a**, **8b**, **9a** and **10a**) reduced cell growth to less than 50% when assayed at 10  $\mu$ M in these cells. Some compounds also matched this threshold in PC-3, CCRF-CEM, HTB-54, MOLT-4 and HT-29 cells. However, none of the derivatives was able to reduce the cell growth effectively in K-562, the most resistant cell line to the treatments. Interestingly, compounds **1b**, **2b**, **4b**, **8a**, **8b**, **9a** and **10a** did not significantly affect cell growth in 184B5 cells, thus suggesting a potential selectivity of the compounds for breast cancer cells. Consequently, those seven compounds were further analysed in full dose-response curves in every cell line.  $GI_{50}$ , TGI and  $LC_{50}$  values were calculated from the curves and are shown in Table 1. Selectivity for tumor cells was estimated according to the formulas  $GI_{50}$  (184B5)/ $GI_{50}$  (MCF-7) and  $GI_{50}$  (BEAS-2B)/ $GI_{50}$  (HTB-54) (Table 2).

As shown in Tables 1 and 2, derivatives **8a**, **9a** and **10a** exhibited  $GI_{50}$  values under 10  $\mu$ M in three of the tested cancer cell lines. Besides, compounds **1b**, **2b**, **4b**, **8b** and **10a** were highly selective for tumor cells in the breast model. Remarkably, though highly

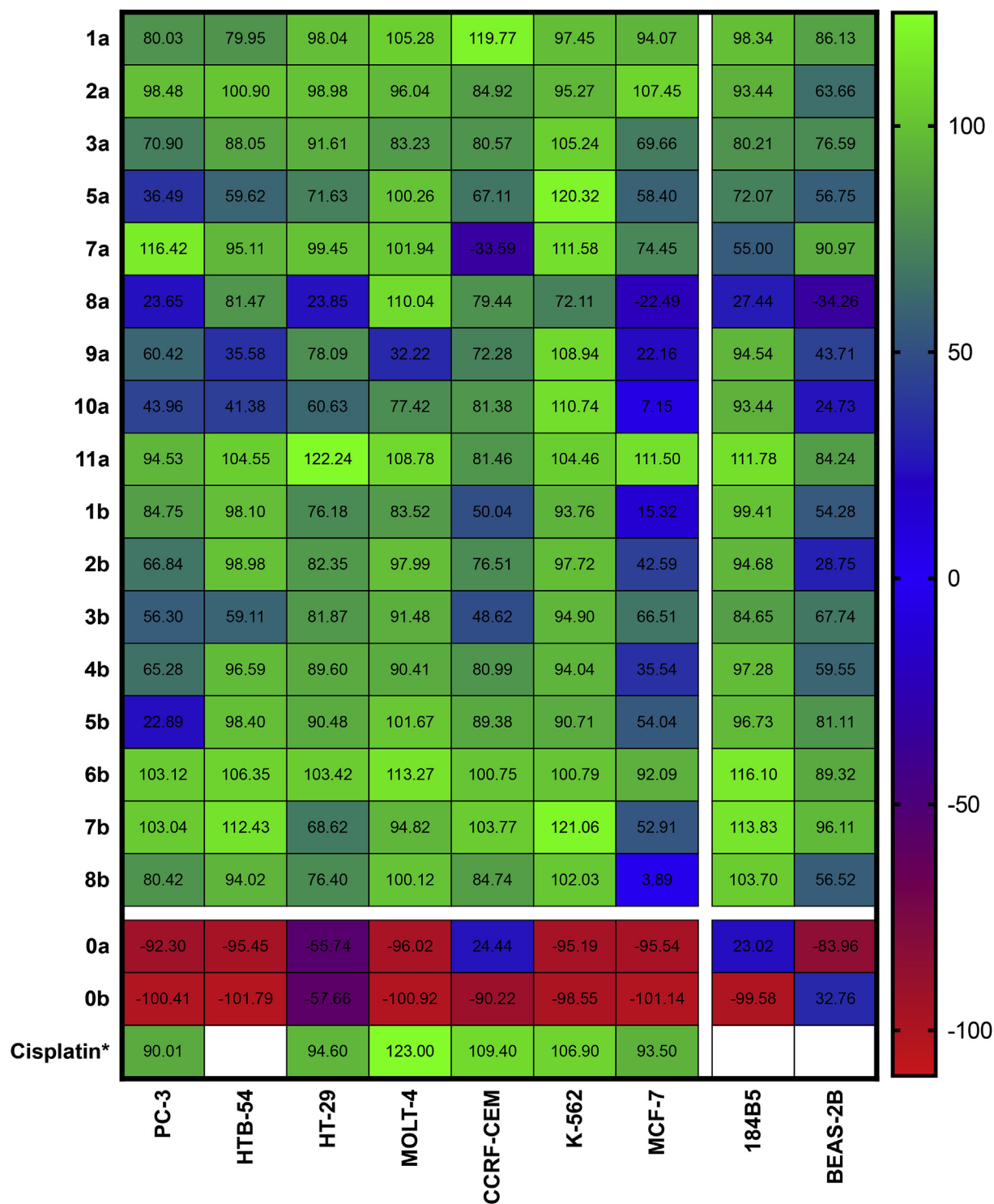


**Fig. 4.** Heat map representing average percentages of cell growth for every tested structure at a 10  $\mu$ M concentration for 48 h  
\* NCI data (<http://dtp.nci.nih.gov>).

cytotoxic, parent compounds **0a** and **0b** showed low selectivity for breast cancer cells ( $SI < 9$ ). Therefore, we decided to focus on the effects of these compounds in the breast cancer cell line. When ranked in terms of potency and selectivity for breast cancer cells, a clear gap established **10a**, a compound with a nanomolar  $GI_{50}$  value and a staggering SI, as the leader structure. Despite less cytotoxic, **1b** and **8b** were also highly selective. Among them, the analog

derivative of norcantharidin (**8b**) was selected in order to evaluate whether this structure was able to mimic norcantharidin's effect and induce autophagy. As a result, derivatives **8b** and **10a** were selected to further analyse their mechanism of action in MCF-7 cells. As only the highest concentration tested led to negative growth values as exemplified on Fig. 5, these results uncover a mainly cytostatic profile.

**Table 1**  
Average values of  $GI_{50}$ , TGI and  $LD_{50}$  ( $\mu M$ ) for 48 h treatment.

Code	PC-3			HTB-54			HT-29			MOLT-4			CCRF-CEM			K-562			MCF-7		
	$GI_{50}^a$	TGI <sup>b</sup>	$LD_{50}^c$	$GI_{50}$	TGI	$LD_{50}$	$GI_{50}$	TGI	$LD_{50}$	$GI_{50}$	TGI	$LD_{50}$	$GI_{50}$	TGI	$LD_{50}$	$GI_{50}$	TGI	$LD_{50}$	$GI_{50}$	TGI	$LD_{50}$
1b	30.44	61.35	92.89	46.95	72.42	93.75	>100	>100	>100	>100	>100	>100	6.77	38.33	91.19	58.58	98.17	>100	1.93	14.83	73.09
2b	19.38	>100	>100	>100	>100	>100	>100	>100	>100	>100	>100	>100	30.16	64.24	95.49	42.82	61.91	88.70	7.71	59.13	>100
4b	68.52	>100	>100	>100	>100	>100	>100	>100	>100	>100	>100	>100	46.52	>100	>100	>100	>100	>100	6.47	>100	>100
8a	4.51	17.03	50.55	27.51	55.94	85.49	5.74	33.38	>100	73.77	84.71	94.62	59.13	75.84	>100	25.32	59.67	94.62	7.50	9.18	11.56
8b	21.05	43.22	70.44	47.83	72.42	>100	11.89	42.82	93.75	59.67	69.80	80.15	68.52	>100	>100	67.89	80.15	92.04	3.33	11.56	>100
9a	13.52	36.61	67.89	8.30	14.29	24.18	14.16	20.67	31.01	7.50	15.67	33.69	20.29	47.39	78.69	48.72	69.80	87.08	6.01	11.89	16.57
10a	8.30	33.08	>100	4.91	51.97	>100	11.67	>100	>100	91.19	>100	>100	>100	>100	>100	80.89	>100	>100	0.00096	7.64	>100
0b	1.02	1.54	2.30	0.87	1.00	1.13	0.27	1.11	5.28	3.33	3.39	3.42	1.71	2.74	4.43	1.03	1.29	1.58	1.00	1.48	2.20
0a	0.80	1.62	2.98	0.21	0.80	2.16	<0.01	1.78	8.37	3.84	5.95	8.06	5.28	16.87	42.82	0.95	1.19	1.48	0.75	0.96	1.16
Cisplatin <sup>e</sup>	5.01	50.1	>100	n.d. <sup>d</sup>	n.d. <sup>d</sup>	n.d. <sup>d</sup>	7.94	>100	>100	1.58	63.10	>100	1.00	79.43	>100	5.01	>100	>100	3.16	>100	>100

<sup>a</sup>  $GI_{50}$  concentration that reduces growth by 50% compared to control.

<sup>b</sup> TGI, concentration that completely inhibits cell growth.

<sup>c</sup>  $LD_{50}$  concentration that kills 50% of cells.

<sup>d</sup> Not determined.

<sup>e</sup> NCI data (<http://dtp.nci.nih.gov>).

**Table 2**

Average values of  $GI_{50}$ , TGI and  $LD_{50}$  ( $\mu M$ ) for 48 h treatment and calculated SI.

Code	184B5			SI <sup>a</sup>	BEAS-2B			SI <sup>b</sup>
	$GI_{50}$	TGI	$LD_{50}$		$GI_{50}$	TGI	$LD_{50}$	
1b	>100	>100	>100	>51.73	10.45	42.82	80.15	0.22
2b	>100	>100	>100	>12.98	4.43	24.63	>100	<0.39
4b	>100	>100	>100	15.46	52.93	>100	>100	<0.16
8a	8.93	11.25	15.67	1.19	1.05	4.43	15.53	0.04
8b	77.25	91.19	>100	23.19	15.82	51.02	77.25	0.33
9a	40.51	63.07	86.29	6.74	1.97	43.62	73.77	0.24
10a	60.78	>100	>100	$6.3 \times 10^4$	0.75	20.86	61.91	0.15
0a	6.29	14.03	30.44	8.39	0.73	0.88	1.09	3.44
0b	0.88	1.06	1.27	0.88	7.92	14.69	27.51	9.06

<sup>a</sup> Selectivity index (SI) calculated as  $GI_{50}$  (184B5)/ $GI_{50}$  (MCF-7).

<sup>b</sup> SI calculated as  $GI_{50}$  (BEAS-2B)/ $GI_{50}$  (HTB-54).

Besides, comparison between **10a** and **0a** clearly showed a great enhancement in selectivity for the second generation compound. In fact, SI was 7,000 times higher for compound **10a** than for **0a**, its parent compound. This effect was less notorious when compound **8b** was compared with **0b**. However, both **10a** and **8b** succeeded in increasing the selectivity towards the cancer cells, thus meeting one of our goals.

The importance of estrogen receptors (ER) in cell cycle and cell proliferation in breast cancer cells, as well as the crucial role of estradiol synthesis pathways has been widely described. In fact, antiestrogens have been found to repress transcription of several ER $\alpha$  target genes in MCF-7 cells, specifically in S phase [35]. Besides, when MCF-7 cell cultures were exposed to a genotoxic agent higher levels of DNA damage in S- and G2/M-enriched cultures correlated with higher levels of CYP1A1 y CYP1B1 [36]. MCF-7 is an ER $\alpha$  expressing cell line. Therefore, to compare we decided to test **8b** and **10a** in MDA-MB-231, a breast cancer cell line non-expressing ER $\alpha$ . Obtained results for MDA-MB-231 cells are shown in Fig. 5. As shown in the figure, **8a** and **10a** dose-response curves in MDA-MB-231 differ from those obtained in MCF-7 cells. Moreover, lying in the micromolar range  $GI_{50}$ , TGI and  $LD_{50}$  values for **8b** ( $GI_{50}$  = 33.61  $\mu M$ , TGI = 61.92  $\mu M$  and  $LD_{50}$  = 83.92  $\mu M$ ) and **10a** ( $GI_{50}$  = 13.65  $\mu M$ , TGI = 51.49  $\mu M$  and  $LD_{50}$  > 100  $\mu M$ ) are also higher than in MCF-7 cells. These data suggest that ER signalling and/or estradiol metabolism play a relevant role in cytostatic effect displayed by **8b** and **10a** in MCF-7 cells.

In terms of structure-activity relationship, most diselenide structures containing carboxylic moieties were discarded in the screening process. For instance, when comparing **8b** with its diselenide homolog a complete loss of selectivity could be observed. On the other hand, if we establish a comparison between carboxylic derivatives and their cyclic imide homologs data suggests that this modification was crucial for both potency and selectivity.

### 2.2.2. Compounds **8b** and **10a** induce cell cycle arrest in S phase and cell death

Many selenium containing compounds involve cell cycle regulation among their therapeutic effects [13]. Therefore, as a first approach to the mechanism of action we studied the effect of **8b** and **10a** on cell cycle. With this purpose, the cell cycle status of MCF-7 cell cultures treated with different concentrations of **8b** and **10a** and for different time points was determined by flow cytometry. Camptothecin was used as positive control. As shown in the Fig. 6, both a reduction in the number of G<sub>0</sub>/G<sub>1</sub> cells and a significant increase in the percentage of cells in S phase were detected for both compounds even at the lowest concentration (10  $\mu M$ ) and the shortest time tested (24 h). This result, indicative of S phase arrest was both dose (Fig. 6A) and time (Fig. 6B and C) dependent.

To study the role of apoptosis in the induction of cell death by **8b**

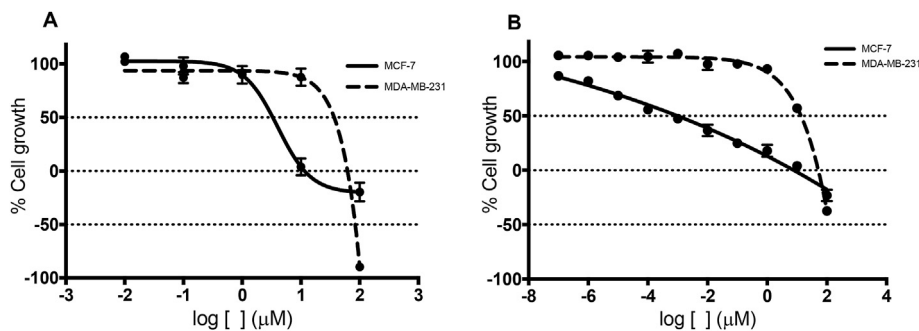


Fig. 5. Dose response curves obtained for 8b (A) and 10a (B) in MCF-7 and MDA-MB-231 cell lines.

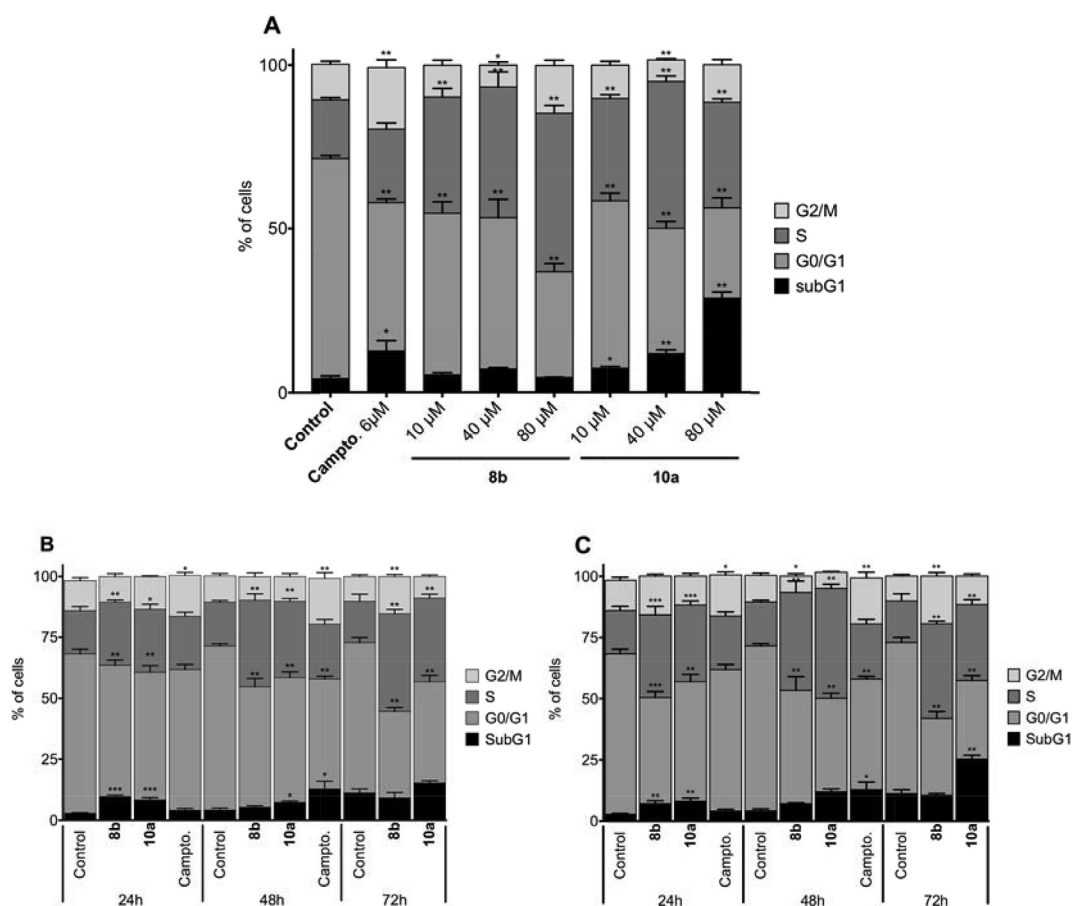


Fig. 6. Cell cycle phase distribution of MCF-7 cell cultures after treatment with compounds **8b** and **10a**. (A) Dose-dependent induction of cell cycle arrest after 48 h treatment with compounds **8b** and **10a**. Time-course analysis of cell cycle distribution at 10  $\mu$ M (B) and 40  $\mu$ M (C) of **8b** and **10a**. Camptothecin (6  $\mu$ M) was employed as a positive control. Results are expressed as a mean  $\pm$  SEM of at least three independent experiments performed in duplicate. \* $p$  < 0.05, \*\* $p$  < 0.01 and \*\*\* $p$  < 0.001 compared to control cells.

and **10a**, MCF-7 cells were incubated in the presence of increasing concentrations of **8b** and **10a** for 48 h. Then, the apoptotic status of the cells was studied by TUNEL. As shown in Fig. 7A, when tested at concentrations higher than 40  $\mu$ M, both compounds induced a significant increase in the number of death cells (subdiploid cells). Fig. 7B shows that at 40  $\mu$ M concentration the induction of cell death could be detected as soon as 24 h.

### 2.2.3. Compounds **8b** and **10a** induce autophagy-mediated cell death and AMPK/JNK pathway activation

To further analyse the molecular mechanism by which **8b** and **10a** reduced MCF-7 cell viability, we explored the effect of pre-

treatment of the cultures with either an autophagy inhibitor (wortmannin, chloroquine) [37–39] or a pan-caspase inhibitor (Z-VAD-FMK) on the induction of cell death by these compounds. As shown in Fig. 8, pre-treatment of the cells with the PI3K inhibitor wortmannin or the lysosomal inhibitor chloroquine led to a significant reduction in the number of dead cells in the cultures after exposure to compounds **8b** and **10a**. However, pre-incubation of the cultures with Z-VAD-FMK could not prevent **8b** and **10a**-induced cell death. These results suggest that autophagy is the way by which **8b** and **10a** cause their effect.

To further confirm the involvement of autophagy in **8b** and **10a** induced cell death the levels of expression of the autophagy

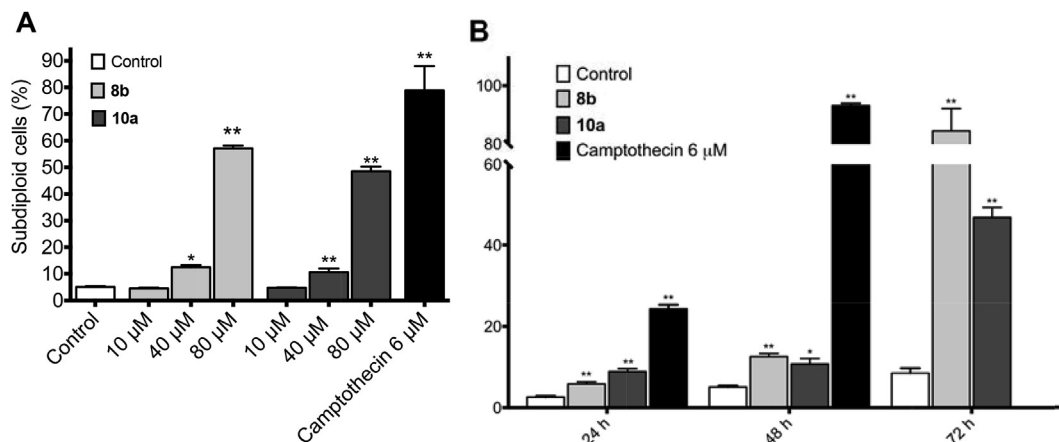


**Fig. 7. Compounds 8b and 10a induced cell death in a dose- and time-dependent manner in MCF-7 cell cultures.** Cells were treated with increasing concentrations of compounds **8b** and **10a** for 48 h (A) or at 40  $\mu\text{M}$  concentration for different periods of time (B). Camptothecin was used as positive control. Results are expressed as a mean  $\pm$  SEM of at least three independent experiments performed in duplicate. \* $p < 0.05$  and \*\* $p < 0.01$  compared to control cells.

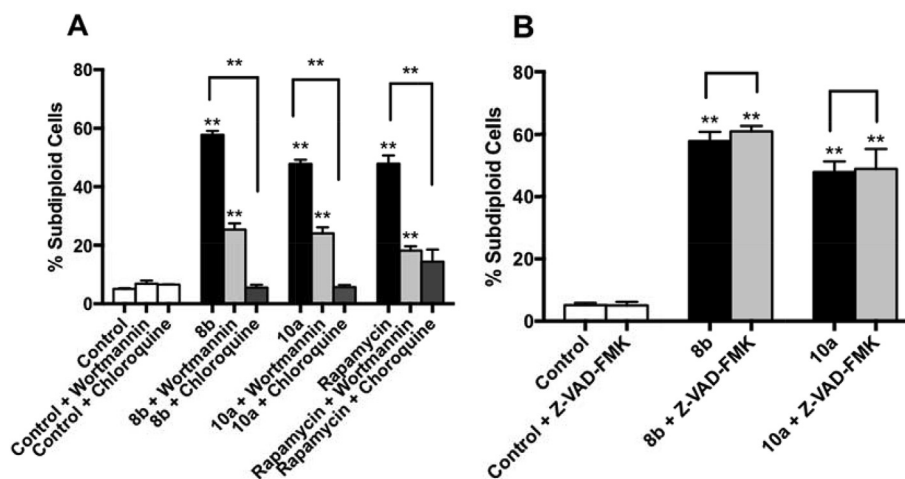


**Fig. 8. Cell death induced by compounds 8b and 10a is partially blocked by wortmannin or chloroquine but not by caspase inhibitor Z-VAD-FMK.** Cell death determination in MCF-7 cell cultures pre-incubated with (A) 100 nM wortmannin, 10  $\mu\text{M}$  chloroquine or (B) 50 mM Z-VAD-FMK before treatment with 80  $\mu\text{M}$  **8b**, 80  $\mu\text{M}$  **10a** or 30  $\mu\text{M}$  rapamycin for 48 h. Rapamycin was used as reference autophagy control at 30  $\mu\text{M}$  treatment. Results are expressed as a mean  $\pm$  SEM of at least three independent experiments performed in duplicate. \* $p < 0.05$  and \*\* $p < 0.01$  compared to the control.

markers Beclin-1 and LC3B were determined. Autophagic flux was also assessed by testing SQSTM1/p62 [40]. As shown in Fig. 9, when MCF-7 cells were treated with 80  $\mu\text{M}$  of either compound for 48 h, Beclin-1, LC3B-I and LC3B-II were augmented while SQSTM1/p62 was downregulated thus confirming autophagy. Since the activation of AMPK and JNK have been shown to play a role in autophagy-mediated cell death [6,41], AMPK and JNK phosphorylation were also studied. As shown in Fig. 9, both **8b** and **10a** induced AMPK and JNK phosphorylation.

Inhibition of mTORC1 after AMPK activation is a main step in AMPK-mediated autophagy. The PI3K/AKT pathway also has a regulatory effect on mTOR and therefore in autophagy. This pathway is commonly deregulated in cancer cells [42]. Aimed to analyze the effect of **8b** and **10a** on PI3K and AKT signaling, we determined the phosphorylation status of both, the PI3K catalytic subunit p110 $\alpha$  and AKT (Ser473). As shown in Fig. 10, increased phospho-p110 $\alpha$  and phospho-AKT (Ser473) were detected indicating activation of the pathway. PI3K activation is usually related to tumor migration enhancement [43] and has been reported to be associated with inhibition of autophagy and tumorigenesis [44].

However, in the specific context of breast adenocarcinoma cells PI3K activation does not necessarily lead to autophagy suppression [45]. Moreover, specific activation of the isoform 1 of AKT in breast, neck and head carcinomas has been shown to interfere with their metastatic progression [46,47]. Whether AKT-mediated repression of metastasis would represent an additional beneficial effect of the treatment with compounds **8b** and **10a** merits further research.

### 3. Conclusion

To sum up, nine diselenide (**1a-3a**, **5a**, **7a-11a**) and eight selenocyanate monoamidic acids (**1b-8b**) were synthesized with high yields. A screening in a panel of cancer cell lines revealed that MCF-7 was the most sensitive among the tested ones to treatment with these compounds. Due to their high potency and stunning selectivity towards MCF-7 cells, derivatives **8b** and **10a** emerged as the most promising structures. Full dose response curves in MCF-7 cells showed up a cytostatic effect for these compounds. Further analysis uncovered their ability to induce both S phase arrest and a caspase-independent cell death program in these cells. Besides,

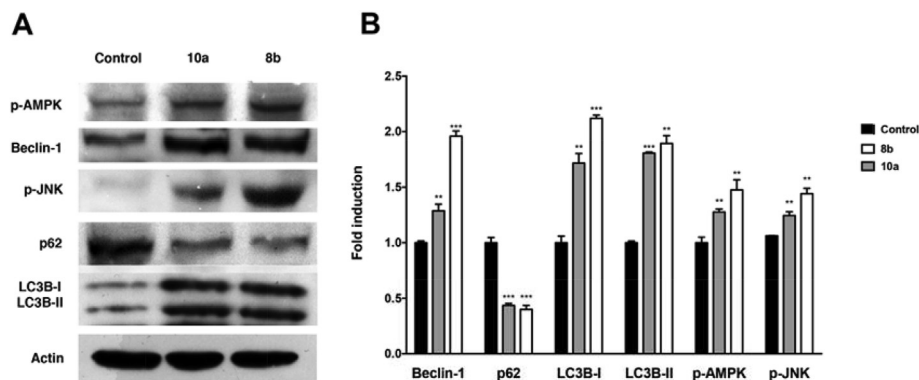


**Fig. 9.** Beclin-1, p62, LC3B-I, LC3B-II, p-AMPK and p-JNK proteins were determined by western blot. (A) A representative experiment is exemplified. (B) Aggregate results (mean  $\pm$  SEM; n = 3) expressed as fold induction relative to control cells. \*p < 0.05, \*\*p < 0.01 and \*\*\*p < 0.001.

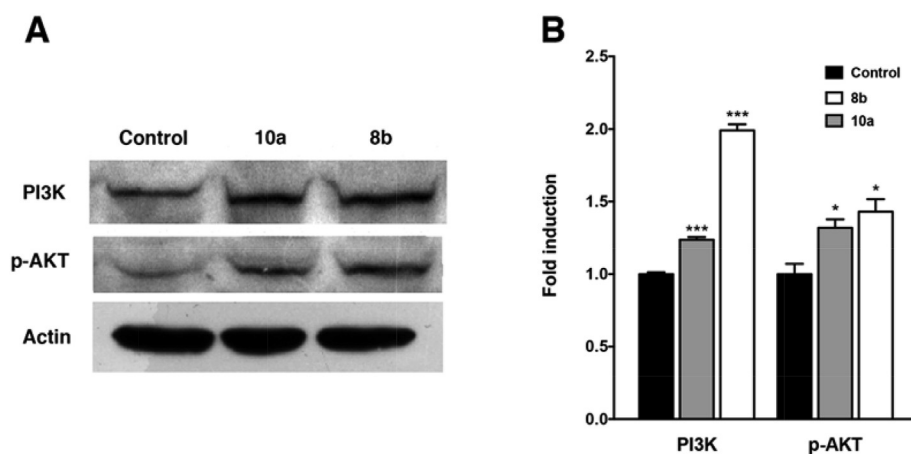


**Fig. 10.** PI3K and p-AKT proteins were determined by western blot. (A) A representative experiment is exemplified. (B) Aggregate results (mean  $\pm$  SEM; n = 3) expressed as fold induction relative to control cells. \*p < 0.05, \*\*p < 0.01 and \*\*\*p < 0.001.

wortmannin and chloroquine partially prevented induction of cell death, thus suggesting autophagy. Increased levels of Beclin1 and LC3-IIB and reduced levels of SQSTM1/p62 in MCF-7 cells after exposure to **8b** or **10a** also supported autophagy. Since pJNK upregulation and AMPK phosphorylation were also detected after the treatments, the modulation of the AMPK and JNK signaling pathways seems to be involved in the induction of autophagy by **8b** and **10a**. Finally, the phosphorylation of both, AKT and the PI3K catalytic subunit p110 $\alpha$  were also detected. Whether the activation of the PI3K/AKT pathway by **8b** and **10a** in MCF-7 cells restricts their invasive capacity and represents an extra beneficial effect of these compounds for cancer treatment deserves to be studied profoundly.

## 4. Experimental

### 4.1. Chemistry

#### 4.1.1. Material and methods

Proton ( $^1\text{H}$ ) and carbon ( $^{13}\text{C}$ ) NMR spectra of every compound and selenium ( $^{77}\text{Se}$ ) NMR spectra of representative derivatives were recorded on a Bruker Advance Neo 400 Ultrashield<sup>TM</sup> spectrometer (Rheinstetten, Germany) using DMSO- $d_6$  as solvent. IR spectra were recorded on a Thermo Nicolet FT-IR Nexus spectrophotometer using KBr pellets for solid samples. Elemental analysis was performed on a LECO CHN-900 Elemental Analyzer. Purity of

all final compounds was 95% or higher. Chemicals were purchased from E. Merck (Darmstadt, Germany), Panreac Química S.A. (Montcada i Reixac, Barcelona, Spain), Sigma-Aldrich Química, S.A. (Alcobendas, Madrid, Spain) and Acros Organics (Janssen Pharmaceutica, Geel, Belgium).

#### 4.1.2. General procedure for the synthesis of compounds **1a-3a**, **5a** and **7a-8a**

Bis(4-aminophenyl)diselenide (1 mmol) was dissolved in dry acetone (10 mL) and the corresponding anhydride (2.1 mmol) then added. The reaction was then stirred for a variable time of 8 h up to 24 h at room temperature. Then reaction was quenched with water, compound was filtered and purified by stirring or washing with ethyl ether.

In order to assign the chemical shifts in NMR spectroscopy the following assignment has been done: central rings A and A', external fragments B and B' (Fig. 11).

4.1.2.1. (2Z,2'Z)-4,4'-[diselenodiy]bis(benzene-4,1-diyimino)]bis(4-oxobut-2-enoic acid) (**1a**). From maleic anhydride. Conditions: 8 h at room temperature. The product was kept under stirring with water (25 mL) for 2 h, filtered and then washed with ethyl ether (2  $\times$  25 mL). A yellow powder was obtained. Yield: 68.9%. Mp: 186–186.5  $^\circ\text{C}$ . IR (KBr)  $\text{cm}^{-1}$ : 3305, 3193 (N–H), 1723 (C=O carboxylic acid), 1623 (C=O, amide), 818 (Se–Se).  $^1\text{H}$  NMR (400 MHz, DMSO- $d_6$ )  $\delta$ : 13.01 (bs, 2H, COOH), 10.54 (s, 2H, NH), 7.60 (d, 4H,

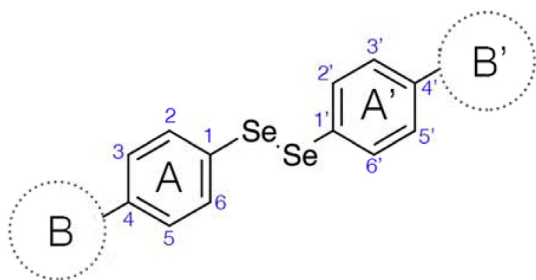


Fig. 11. General NMR assignation for compounds of series a.

A + A',  $J_{2-3}=J_{6-5}=8.8$  Hz, H<sub>2</sub>+H<sub>6</sub>), 7.57 (d, 4H, A + A',  $J_{3-2}=J_{5-6}=8.8$  Hz, H<sub>3</sub>+H<sub>5</sub>), 6.46 (d, 2H, B + B',  $J_{1-2}=12.0$  Hz, H<sub>1</sub>), 6.31 (d, 2H, B + B',  $J_{2-1}=12.0$  Hz, H<sub>2</sub>). <sup>13</sup>C NMR (100 MHz, DMSO-*d*<sub>6</sub>) δ: 166.76 (COOH), 163.17 (C=O), 138.71 (A + A', C<sub>4</sub>), 132.88 (A + A', C<sub>2</sub>+C<sub>6</sub>), 131.33 + 130.23 (B + B', C<sub>1</sub>+C<sub>2</sub>), 124.19 (A + A', C<sub>1</sub>), 120.02 (A + A', C<sub>3</sub>+C<sub>5</sub>). MS [*m/z* (% abundance)]: 172 (100), 344 (25). Elemental analysis calculated (%) for C<sub>20</sub>H<sub>16</sub>N<sub>2</sub>O<sub>6</sub>Se<sub>2</sub> · 2H<sub>2</sub>O: C: 41.83, H: 3.51, N: 4.88; found: C: 41.54, H: 3.53, N: 4.80.

4.1.2.2. 2,2'-[(Diselenodiyldibenzene-4,1-diyl)dicarbamoyl]bis(benzoic acid) (**2a**). From phthalic anhydride. Conditions: 12 h at room temperature. The product was kept under stirring with water (25 mL) for 1 h, filtered and then washed with ethyl ether (2 × 25 mL). A yellow powder was obtained. Yield: 26.7%. Mp: 154–155 °C. IR (KBr) cm<sup>-1</sup>: 3282 (N–H), 1708 (C=O carboxylic acid), 1657 (C=O, amide), 819 (Se–Se). <sup>1</sup>H NMR (400 MHz, DMSO-*d*<sub>6</sub>) δ: 11.02 (s, 2H, NH), 7.85 (d, 2H, B + B',  $J_{3-4}=8.8$  Hz, H<sub>3</sub>), 7.72–7.66 (m, 4H, B + B', H<sub>4</sub>+H<sub>6</sub>), 7.63–7.52 (m, 10H, A + A', H<sub>2</sub>+H<sub>3</sub>+H<sub>4</sub>+H<sub>5</sub>, B + B', H<sub>5</sub>), 3.39 (bs, H<sub>2</sub>O+2COOH). <sup>13</sup>C NMR (100 MHz, DMSO-*d*<sub>6</sub>) δ: 171.22 (COOH), 168.50 (C=O), 140.48 (A + A', C<sub>4</sub>), 134.06 + 132.02 (A + A', C<sub>2</sub>+C<sub>6</sub>+C<sub>1</sub>), 130.40 + 130.27 (B + B', C<sub>5</sub>+C<sub>4</sub>), 128.65 + 126.48 (B + B', C<sub>1</sub>+C<sub>2</sub>), 124.60 (A + A', C<sub>3</sub>+C<sub>5</sub>), 121.03 + 120.51 (B + B', C<sub>3</sub>+C<sub>6</sub>). <sup>77</sup>Se NMR (76 MHz, DMSO-*d*<sub>6</sub>) δ: 482.83 (Se–Se). MS [*m/z* (% abundance)]: 104 (100), 172 (93), 344 (25). Elemental analysis calculated (%) for C<sub>28</sub>H<sub>20</sub>N<sub>2</sub>O<sub>6</sub>Se<sub>2</sub> · 2H<sub>2</sub>O: C: 49.87, H: 3.59, N: 4.15; found: C: 49.73, H: 3.53, N: 4.35.

4.1.2.3. 4,4'-[Diselenodiyldibis(benzene-4,1-diylimino)]bis(4-oxobutanoic acid) (**3a**). From succinic anhydride. Conditions: 24 h at room temperature. The product was kept under stirring with water (25 mL) for 2 h, filtered, then stirred with ethyl ether (100 mL) for 24 h and then filtered. A yellow powder was obtained. Yield: 72.27%. Mp: 179–180 °C. IR (KBr) cm<sup>-1</sup>: 3318 (NH), 1696 (C=O carboxylic acid), 1666 (C=O, amide), 818 (Se–Se). <sup>1</sup>H NMR (400 MHz, DMSO-*d*<sub>6</sub>) δ: 12.21 (bs, 2H, COOH), 10.11 (s, 2H, NH), 7.56 (d, 4H, A + A',  $J_{2-3}=J_{6-5}=8.4$  Hz, H<sub>2</sub>+H<sub>6</sub>), 7.51 (d, 4H, A + A',  $J_{3-2}=J_{5-6}=8.4$  Hz, H<sub>3</sub>+H<sub>5</sub>), 2.60–2.46 (m, 8H, B + B', H<sub>1</sub>+H<sub>2</sub>). <sup>13</sup>C NMR (100 MHz, DMSO-*d*<sub>6</sub>) δ: 174.27 (COOH), 170.80 (C=O), 140.09 (A + A', C<sub>4</sub>), 133.76 (A + A', C<sub>2</sub>+C<sub>6</sub>), 123.85 (A + A', C<sub>1</sub>), 120.12 (A + A', C<sub>3</sub>+C<sub>5</sub>), 31.57 + 29.23 (B + B', C<sub>2</sub>+C<sub>1</sub>). MS [*m/z* (% abundance)]: 172 (100), 344 (15), 424 (10). Elemental analysis calculated (%) for C<sub>20</sub>H<sub>20</sub>N<sub>2</sub>O<sub>6</sub>Se<sub>2</sub> · 2H<sub>2</sub>O: C: 41.51, H: 4.18, N: 4.84; found: C: 41.11, H: 3.79, N: 4.77.

4.1.2.4. 2,2'-[(Diselenodiyldibis(benzene-4,1-diylimino)]bis(2-oxoethane-2,1-diyl)oxy)diacetic acid (**5a**). From diglycolic anhydride. Conditions: 24 h at room temperature. The product was kept under stirring with water (25 mL) for 2 h, filtered, then stirred with ethyl ether (100 mL) for 24 h and then filtered. A yellow powder was obtained. Yield: 69.7%. Mp: 140–141 °C. IR (KBr) cm<sup>-1</sup>: 3337 (NH), 1709 (C=O carboxylic acid), 1683 (C=O, amide), 818 (Se–Se). <sup>1</sup>H

NMR (400 MHz, DMSO-*d*<sub>6</sub>) δ: 12.76 (bs, 2H, COOH), 10.09 (s, 2H, NH), 7.62 (d, 4H, A + A',  $J_{2-3}=J_{6-5}=8.5$  Hz, H<sub>2</sub>+H<sub>6</sub>), 7.55 (d, 4H, A + A',  $J_{3-2}=J_{5-6}=8.5$  Hz, H<sub>3</sub>+H<sub>5</sub>), 4.19 (s, 4H, B + B', H<sub>1</sub>), 4.17 (s, 4H, B + B', H<sub>2</sub>). <sup>13</sup>C NMR (100 MHz, DMSO-*d*<sub>6</sub>) δ: 172.68 (COOH), 168.99 (C=O), 139.56 (A + A', C<sub>4</sub>), 133.94 (A + A', C<sub>2</sub>+C<sub>6</sub>), 125.01 (A + A', C<sub>1</sub>), 121.22 (A + A', C<sub>3</sub>+C<sub>5</sub>), 71.38 + 69.11 (B + B', C<sub>2</sub>+C<sub>1</sub>). MS [*m/z* (% abundance)]: 93 (95), 172 (100). Elemental analysis calculated (%) for C<sub>20</sub>H<sub>20</sub>N<sub>2</sub>O<sub>8</sub>Se<sub>2</sub>: C: 41.83, H: 3.51, N: 4.88; found: C: 41.83, H: 3.82, N: 5.19.

4.1.2.5. 2,2'-[(Diselenodiyldibenzene-4,1-diyl)dicarbamoyl]bis(cyclohexanecarboxylic acid) (**7a**). From *cis*-1,2-cyclohexanecarboxylic anhydride. Conditions: 24 h at room temperature. The product was kept under stirring with water (25 mL) for 2 h, filtered, then stirred with ethyl ether (100 mL) for 24 h and then filtered. A light brown powder was obtained. Yield: 97.7%. Mp: 150–151 °C. IR (KBr) cm<sup>-1</sup>: 3307 (NH), 1698 (C=O carboxylic acid), 1665 (C=O, amide), 820 (Se–Se). <sup>1</sup>H NMR (400 MHz, DMSO-*d*<sub>6</sub>) δ: 11.88 (bs, 2H, COOH), 9.87 (s, 2H, NH), 7.55 (d, 4H, A + A',  $J_{2-3}=J_{6-5}=8.8$  Hz, H<sub>2</sub>+H<sub>6</sub>), 7.50 (d, 4H, A + A',  $J_{3-2}=J_{5-6}=8.8$  Hz, H<sub>3</sub>+H<sub>5</sub>), 2.93 (d, 2H, B + B',  $J_{1-CH_{chex}}=5.4$  Hz, H<sub>1</sub>), 2.70–2.56 (m, 2H, B + B', H<sub>chex</sub>), 2.09 (d, 2H, B + B',  $J_{CH_{chex-1}}=5.4$  Hz, H<sub>chex</sub>), 1.98 (d, 2H, B + B',  $J=8.9$  Hz, H<sub>chex</sub>), 1.83–1.57 (m, 6H, B + B', 3H<sub>chex</sub>), 1.48–1.24 (m, 6H, B + B', 3H<sub>chex</sub>). <sup>13</sup>C NMR (100 MHz, DMSO-*d*<sub>6</sub>) δ: 175.56 (COOH), 173.36 (C=O), 140.42 (A + A', C<sub>4</sub>), 133.78 (A + A', C<sub>2</sub>+C<sub>6</sub>), 123.66 (A + A', C<sub>1</sub>), 120.26 (A + A', C<sub>3</sub>+C<sub>5</sub>), 43.00 + 42.44 (B + B', C<sub>1</sub>+C<sub>2</sub>), 28.13 + 25.62+24.47 + 22.78 (B + B', C<sub>3</sub>+C<sub>4</sub>+C<sub>5</sub>+C<sub>6</sub>). MS [*m/z* (% abundance)]: 81 (70), 172 (100), 344 (25). Elemental analysis calculated (%) for C<sub>28</sub>H<sub>32</sub>N<sub>2</sub>O<sub>6</sub>Se<sub>2</sub>: C: 51.70, H: 4.96, N: 4.31; found: C: 52.06, H: 5.09, N: 4.71.

4.1.2.6. 3,3'-[(Diselenodiyldibenzene-4,1-diyl)dicarbamoyl]bis(7-oxabicyclo[2.2.1]hept-5-ene-2-carboxylic acid) (**8a**). From 3,6-epoxy-1,2,3,6-tetrahydrophthalic anhydride obtained by the classic procedure described for a Diels-Alder reaction using furan and maleic anhydride as reagents to yield the Diels-Alder adduct. Conditions: 24 h at room temperature. The product was kept under stirring with water (25 mL) for 2 h, filtered, then stirred with ethyl ether (100 mL) for 24 h and then filtered. A yellow powder was obtained. Yield: 22.5%. Mp: 126–127 °C. IR (KBr) cm<sup>-1</sup>: 3299 (NH), 1706 (C=O carboxylic acid), 1669 (C=O, amide), 819 (Se–Se). <sup>1</sup>H NMR (400 MHz, DMSO-*d*<sub>6</sub>) δ: 12.19 (bs, 2H, COOH), 10.03 (s, 2H, NH), 7.65 (d, 4H, A + A',  $J_{2-3}=J_{6-5}=9.0$  Hz, H<sub>2</sub>+H<sub>6</sub>), 7.62 (d, 4H, A + A',  $J_{3-2}=J_{5-6}=9.0$  Hz, H<sub>3</sub>+H<sub>5</sub>), 6.50 (s, 4H, B + B', H<sub>3</sub>+H<sub>5</sub>), 5.14 (s, 2H, B + B', H<sub>5</sub>), 5.06 (s, 2H, B + B', H<sub>2</sub>), 2.82 (d, 2H, B + B',  $J_{1-6}=9.1$  Hz, H<sub>1</sub>), 2.71 (d, 2H, B + B',  $J_{6-1}=9.1$  Hz, H<sub>6</sub>). <sup>13</sup>C NMR (100 MHz, DMSO-*d*<sub>6</sub>) δ: 173.08 (COOH), 170.48 (C=O), 141.07 (A + A', C<sub>4</sub>), 137.49 + 137.08 (B + B', C<sub>4</sub>+C<sub>5</sub>), 135.29 (A + A', C<sub>2</sub>+C<sub>6</sub>), 120.79 (A + A', C<sub>1</sub>), 116.51 (A + A', C<sub>3</sub>+C<sub>5</sub>), 80.82 + 79.61 (B + B', C<sub>3</sub>+C<sub>6</sub>), 47.96 + 47.36 (B + B', C<sub>1</sub>+C<sub>2</sub>). MS [*m/z* (% abundance)]: 172 (100), 344 (25). Elemental analysis calculated (%) for C<sub>28</sub>H<sub>24</sub>N<sub>2</sub>O<sub>8</sub>Se<sub>2</sub> · 2H<sub>2</sub>O: C: 47.34, H: 3.97, N: 3.94; found: C: 47.66, H: 4.13, N: 4.23.

#### 4.1.3. General procedure for the synthesis of compounds **9a–11a**

A reaction mixture containing 1.3 mmol of the corresponding carboxylic derivatives (**1a**, **2a** or **5a**) in 15 mL of acetic anhydride and 200 mg of sodium acetate was heated for 3 h under reflux, then quenched with water (50 mL) and kept under stirring for 3 h. The aqueous solution was extracted with CH<sub>2</sub>Cl<sub>2</sub> (2 × 25 mL), dried with sodium sulphate anhydrous and the solvent was evaporated under vacuum.

4.1.3.1. 1,1'-[Diselenodiyldibenzene-4,1-diyl]bis(1H-pyrrole-2,5-dione) (**9a**). From compound **1a**. The product was then washed

with *n*-hexane (100 mL). A yellow solid was obtained. Yield: 55.4%. Mp: 91.5–92.5 °C. IR (KBr)  $\text{cm}^{-1}$ : 1710 (C=O), 818 (Se–Se).  $^1\text{H}$  NMR (400 MHz, DMSO- $d_6$ )  $\delta$ : 7.77 (d, 4H, A + A',  $J_{2-3} = J_{6-5} = 8.6$  Hz, H<sub>2</sub>+H<sub>6</sub>), 7.33 (d, 4H, A + A',  $J_{3-2} = J_{5-6} = 8.6$  Hz, H<sub>3</sub>+H<sub>5</sub>), 7.19 (s, 4H, B + B', H<sub>1</sub>+H<sub>2</sub>).  $^{13}\text{C}$  NMR (100 MHz, DMSO- $d_6$ )  $\delta$ : 169.69 (C=O), 134.75 (A + A', C<sub>4</sub>), 131.37 + 131.27 (A + A', C<sub>2</sub>+C<sub>6</sub>; B + B', C<sub>1</sub>+C<sub>2</sub>), 129.15 (A + A', C<sub>1</sub>), 127.51 (A + A', C<sub>3</sub>+C<sub>5</sub>). MS [ $m/z$  (% abundance)]: 57 (75), 252 (100), 311 (65). Elemental analysis calculated (%) for C<sub>20</sub>H<sub>12</sub>N<sub>2</sub>O<sub>4</sub>Se<sub>2</sub> · H<sub>2</sub>O: C: 46.17, H: 2.71, N: 5.38; found: C: 46.10, H: 3.03, N: 4.94.

4.1.3.2. 1,1'-(Diselenodiyldibenzene-4,1-diyl)bis(1*H*-isoindole-1,3(2*H*)-dione) (**10a**). From compound **2a**. The product was then washed with *n*-hexane (100 mL). A yellow solid was obtained. Yield: 90.6%. Mp: 248–249 °C. IR (KBr)  $\text{cm}^{-1}$ : 1709 (C=O), 815 (Se–Se).  $^1\text{H}$  NMR (400 MHz, DMSO- $d_6$ )  $\delta$ : 8.15–7.79 (m, 12H, A + A', H<sub>2</sub>+H<sub>6</sub>; B + B', H<sub>2</sub>+H<sub>3</sub>+H<sub>4</sub>+H<sub>5</sub>), 7.55 (d, 4H, A + A',  $J_{3-2} = J_{5-6} = 8.4$  Hz, H<sub>3</sub>+H<sub>5</sub>).  $^{13}\text{C}$  NMR (100 MHz, DMSO- $d_6$ )  $\delta$ : 172.73 (C=O), 140.18 + 140.09 (A + A', C<sub>4</sub>; B + B', C<sub>1</sub>+C<sub>6</sub>), 133.49 (B + B', C<sub>4</sub>+C<sub>5</sub>), 131.99 + 131.73 (A + A', C<sub>1</sub>+C<sub>2</sub>+C<sub>6</sub>), 128.65 (B + B', C<sub>2</sub>+C<sub>5</sub>), 120.26 (A + A', C<sub>3</sub>+C<sub>5</sub>).  $^{77}\text{Se}$  NMR (76 MHz, DMSO- $d_6$ )  $\delta$ : 481.88 (Se–Se). MS [ $m/z$  (% abundance)]: 93 (65), 172 (100), 302 (15), 604 (5). Elemental analysis calculated (%) for C<sub>28</sub>H<sub>16</sub>N<sub>2</sub>O<sub>4</sub>Se<sub>2</sub> · 2H<sub>2</sub>O: C: 52.68, H: 3.16, N: 4.39; found: C: 52.82, H: 3.20, N: 4.77.

4.1.3.3. 1,1'-(Diselenodiyldibenzene-4,1-diyl)bis(morpholine-3,5-dione) (**11a**). From compound **5a**. The product was then washed with ethyl ether (3 × 10 mL). A yellow solid was obtained. Yield: 72.6%. MP: 150–152. IR (KBr)  $\text{cm}^{-1}$ : 1708 (C=O), 819 (Se–Se).  $^1\text{H}$  NMR (400 MHz, DMSO- $d_6$ )  $\delta$ : 7.76 (d, 4H, A + A',  $J_{2-3} = J_{6-5} = 7.8$  Hz, H<sub>2</sub>+H<sub>6</sub>), 7.23 (d, 4H, A + A',  $J_{3-2} = J_{5-6} = 7.8$  Hz, H<sub>3</sub>+H<sub>5</sub>), 4.54 (s, 8H, B + B', H<sub>2</sub>+H<sub>3</sub>).  $^{13}\text{C}$  NMR (100 MHz, DMSO- $d_6$ )  $\delta$ : 170.19 (C=O), 133.32 (A + A', C<sub>4</sub>), 131.42 (A + A', C<sub>2</sub>+C<sub>6</sub>), 130.71 (A + A', C<sub>1</sub>), 130.30 (A + A', C<sub>3</sub>+C<sub>5</sub>), 67.74 (B + B', C<sub>1</sub>+C<sub>2</sub>). MS [ $m/z$  (% abundance)]: 184 (100), 271 (25), 538 (15). Elemental analysis calculated (%) for C<sub>20</sub>H<sub>16</sub>N<sub>2</sub>O<sub>6</sub>Se<sub>2</sub> · H<sub>2</sub>O: C: 43.18, H: 3.26, N: 5.04; found: C: 43.45, H: 3.52, N: 5.36.

#### 4.1.4. General procedure for the synthesis of compounds **1b–8b**

4-Aminophenyl selenocyanate (2 mmol) was dissolved in dry acetone (15 mL) and the corresponding anhydride (2 mmol) then added. The reaction was then stirred for a variable time of 12 h up to 48 h at room temperature. Reaction was quenched with water, compound was then filtered and purified by stirring or washing with solvents such as *n*-hexane and ethyl ether. The chemical shifts assignment in NMR spectroscopy for these compounds is exemplified in Fig. 12.

4.1.4.1. (2*Z*)-4-oxo-4-[(4-selenocyanatophenyl)amino]but-2-enoic acid (**1b**). From maleic anhydride. Conditions: 14 h at room temperature. The product was kept under stirring with water (25 mL) for 2 h, filtered and then washed with *n*-hexane (25 mL) and ethyl ether (25 mL). A yellow powder was obtained. Yield: 51.8%. Mp: 161–162 °C. IR (KBr)  $\text{cm}^{-1}$ : 3299, 3196 (N–H), 2157 (CN), 1722 (C=O carboxylic acid), 1624 (C=O, amide).  $^1\text{H}$  NMR (400 MHz, DMSO- $d_6$ )  $\delta$ : 12.96 (s, 1H, COOH), 10.58 (s, 1H, NH), 7.69 (bs, 4H, A,

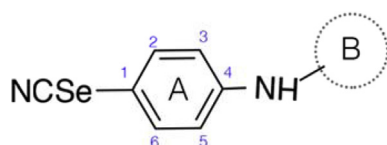


Fig. 12. NMR assignation rules followed for series b.

H<sub>2</sub>+H<sub>3</sub>+H<sub>5</sub>+H<sub>6</sub>), 6.47 (d, 1H, B,  $J_{1-2} = 12.0$  Hz, H<sub>1</sub>), 6.33 (d, 1H, B,  $J_{2-1} = 12.0$  Hz, H<sub>2</sub>).  $^{13}\text{C}$  NMR (100 MHz, DMSO- $d_6$ )  $\delta$ : 167.37 (COOH), 164.02 (C=O), 140.42 (A, C<sub>4</sub>), 135.24 (A, C<sub>2</sub>+C<sub>6</sub>), 132.04 + 130.75 (B, C<sub>1</sub>+C<sub>2</sub>), 121.16 (A, C<sub>3</sub>+C<sub>5</sub>), 117.57 (A, C<sub>1</sub>), 105.77 (CN).  $^{77}\text{Se}$  NMR (76 MHz, DMSO- $d_6$ )  $\delta$ : 322.45 (SeCN). MS [ $m/z$  (% abundance)]: 118 (100), 198 (25), 278 (10), 296 (7). Elemental analysis calculated (%) for C<sub>11</sub>H<sub>8</sub>N<sub>2</sub>O<sub>3</sub>Se: C: 44.74, H: 2.73, N: 9.49; found: C: 44.35, H: 3.08, N: 9.10.

4.1.4.2. 2-[(4-selenocyanatophenyl)carbamoyl]benzoic acid (**2b**). From phthalic anhydride. Conditions: 14 h at room temperature. The product was kept under stirring with water (25 mL) for 2 h, filtered and then washed with *n*-hexane (25 mL) and ethyl ether (25 mL). A white powder was obtained. Yield: 89.5%. Mp: 162–164 °C. IR (KBr)  $\text{cm}^{-1}$ : 3317, 3122 (N–H), 2149 (CN), 1718 (C=O carboxylic acid), 1647 (C=O, amide).  $^1\text{H}$  NMR (400 MHz, DMSO- $d_6$ )  $\delta$ : 13.14 (s, 1H, COOH), 10.60 (s, 1H, NH), 7.92 (d, 1H, B,  $J_{3-4} = 7.5$  Hz, H<sub>3</sub>), 7.78 (d, 2H, A,  $J_{2-3} = J_{6-5} = 8.3$  Hz, H<sub>2</sub>+H<sub>6</sub>), 7.73–7.64 (m, 3H, A, H<sub>3</sub>+H<sub>5</sub>, B, H<sub>4</sub>), 7.62–7.54 (m, 2H, B, H<sub>5</sub>+H<sub>6</sub>).  $^{13}\text{C}$  NMR (100 MHz, DMSO- $d_6$ )  $\delta$ : 168.23 (COOH), 167.80 (C=O), 141.32 + 139.03 (A, C<sub>4</sub>; B, C<sub>1</sub>), 135.29 (A, C<sub>2</sub>+C<sub>6</sub>), 132.31 (B, C<sub>5</sub>), 130.30 + 130.09+130.05 (B, C<sub>2</sub>+C<sub>3</sub>+C<sub>4</sub>), 128.25 (B, C<sub>6</sub>), 121.16 (A, C<sub>1</sub>), 116.99 (A, C<sub>3</sub>+C<sub>5</sub>), 105.91 (CN). MS [ $m/z$  (% abundance)]: 76 (50), 104 (55), 118 (100), 198 (20). Elemental analysis calculated (%) for C<sub>15</sub>H<sub>10</sub>N<sub>2</sub>O<sub>3</sub>Se: C: 52.19, H: 2.92, N: 8.11; found: C: 52.06, H: 3.24, N: 8.06.

4.1.4.3. 4-Oxo-4-[(4-selenocyanatophenyl)amino]butanoic acid (**3b**). From succinic anhydride. Conditions: 24 h at room temperature. The product was kept under stirring with water (25 mL) for 2 h, filtered, then stirred with ethyl ether (100 mL) for 24 h and then filtered. A brown powder was obtained. Yield: 36.7%. Mp: 154–156 °C. IR (KBr)  $\text{cm}^{-1}$ : 3340 (NH), 2158 (CN), 1693 (C=O carboxylic acid), 1636 (C=O, amide).  $^1\text{H}$  NMR (400 MHz, DMSO- $d_6$ )  $\delta$ : 12.18 (bs, 1H, COOH), 10.21 (s, 1H, NH), 7.66 (bs, 4H, A, H<sub>2</sub>+H<sub>6</sub>+H<sub>3</sub>+H<sub>5</sub>), 2.58 (d, 2H, A,  $J_{2-1} = 6.0$  Hz, H<sub>2</sub>), 2.54 (d, 2H, A,  $J_{1-2} = 6.0$  Hz, H<sub>1</sub>).  $^{13}\text{C}$  NMR (100 MHz, DMSO- $d_6$ )  $\delta$ : 174.27 (COOH), 171.03 (C=O), 141.06 (A, C<sub>4</sub>), 135.36 (A, C<sub>2</sub>+C<sub>6</sub>), 120.60 (A, C<sub>3</sub>+C<sub>5</sub>), 116.47 (A, C<sub>1</sub>), 105.90 (CN), 31.54 (B, C<sub>2</sub>), 29.10 (B, C<sub>1</sub>). MS [ $m/z$  (% abundance)]: 101 (25), 118 (100), 198 (40), 298 (28). Elemental analysis calculated (%) for C<sub>11</sub>H<sub>10</sub>N<sub>2</sub>O<sub>3</sub>Se<sub>2</sub> · H<sub>2</sub>O: C: 41.92, H: 3.84, N: 8.89; found: C: 41.59, H: 3.58, N: 8.69.

4.1.4.4. 3-[(4-selenocyanatophenyl)carbamoyl]pyrazine-2-carboxylic acid (**4b**). From 2,3-pyrazinedicarboxylic anhydride. Conditions: 24 h at room temperature. The product was kept under stirring with water (25 mL) for 3 h, filtered, then stirred with ethyl ether (100 mL) for 24 h and then filtered. A yellow powder was obtained. Yield: 49.3%. Mp: 164–165 °C. IR (KBr)  $\text{cm}^{-1}$ : 3280 (NH), 2153 (CN), 1765 (C=O carboxylic acid), 1671 (C=O, amide).  $^1\text{H}$  NMR (400 MHz, DMSO- $d_6$ )  $\delta$ : 13.82 (bs, 1H, COOH), 11.03 (s, 1H, NH), 8.92 (s, 2H, B, H<sub>3</sub>+H<sub>4</sub>), 7.87 (d, 2H, A,  $J_{2-3} = J_{6-5} = 8.6$  Hz, H<sub>2</sub>+H<sub>6</sub>), 7.74 (d, 2H, A,  $J_{3-2} = J_{5-6} = 8.6$  Hz, H<sub>3</sub>+H<sub>5</sub>).  $^{13}\text{C}$  NMR (100 MHz, DMSO- $d_6$ )  $\delta$ : 167.05 (COOH), 163.64 (C=O), 146.99 + 146.75+146.15 + 145.49 (B, C<sub>1</sub>+C<sub>2</sub>+C<sub>3</sub>+C<sub>4</sub>), 140.49 (A, C<sub>4</sub>), 135 (A, C<sub>2</sub>+C<sub>6</sub>), 122.19 (A, C<sub>3</sub>+C<sub>5</sub>), 118 (A, C<sub>1</sub>), 106.37 (CN). MS [ $m/z$  (% abundance)]: 79 (100), 107 (95), 118 (30), 304 (75). Elemental analysis calculated (%) for C<sub>13</sub>H<sub>8</sub>N<sub>4</sub>O<sub>3</sub>Se: C: 44.97, H: 2.32, N: 16.14; found: C: 44.73, H: 2.72, N: 15.82.

4.1.4.5. {2-Oxo-2-[(4-selenocyanatophenyl)amino]ethoxy}acetic acid (**5b**). From diglycolic anhydride. Conditions: 24 h at room temperature. The product was kept under stirring with water (25 mL) for 1 h, filtered and then washed with ethyl ether (2 × 25 mL). A white powder was obtained. Yield: 51.1%. Mp: 141–142 °C. IR (KBr)  $\text{cm}^{-1}$ : 3305 (NH), 2151 (CN), 1716 (C=O carboxylic acid), 1660 (C=O, amide).  $^1\text{H}$  NMR (400 MHz, DMSO- $d_6$ )  $\delta$ : 12.91 (bs, 1H, COOH), 10.14

(s, 1H, NH), 7.74 (d, 2H, A,  $J_{2-3} = J_{6-5} = 8.8$  Hz,  $H_2+H_6$ ), 7.68 (d, 2H, A,  $J_{3-2} = J_{5-6} = 8.8$  Hz,  $H_3+H_5$ ), 4.21 (s, 2H, B,  $H_1$ ), 4.20 (s, 2H, B,  $H_2$ ).  $^{13}\text{C}$  NMR (100 MHz, DMSO- $d_6$ )  $\delta$ : 172.25 (COOH), 168.78 (C=O), 140.14 (A,  $C_4$ ), 135.27 (A,  $C_2+C_6$ ), 121.30 (A,  $C_3+C_5$ ), 117.43 (A,  $C_1$ ), 105.92 (CN), 70.83 (B,  $C_1$ ), 68.51 (B,  $C_2$ ). MS [ $m/z$  (% abundance)]: 118 (85), 198 (40), 211 (30), 314 (100). Elemental analysis calculated (%) for  $\text{C}_{11}\text{H}_{10}\text{N}_2\text{O}_4\text{Se}$ : C: 42.19, H: 3.22, N: 8.95; found: C: 41.92, H: 3.53, N: 8.82.

**4.1.4.6. 2'-[(4-Selenocyanatophenyl)carbamoyl]-[1,1'-biphenyl]-2-carboxylic acid (6b).** From diphenic anhydride. Conditions: 48 h at room temperature. The product was kept under stirring with water (25 mL) for 3 h, filtered and then washed with ethyl ether (2  $\times$  25 mL). A white powder was obtained. Yield: 21.8%. Mp: 146–147 °C. IR (KBr)  $\text{cm}^{-1}$ : 3296 (NH), 2153 (CN), 1726 (C=O, carboxylic acid), 1631 (C=O, amide).  $^1\text{H}$  NMR (400 MHz, DMSO- $d_6$ )  $\delta$ : 12.80 (bs, 1H, COOH), 10.24 (s, 1H, NH), 7.83 (d, 1H, B,  $J_{9-10} = 7.6$  Hz,  $H_9$ ), 7.67–7.58 (m, 3H, B,  $H_2+H_5+H_{12}$ ), 7.58–7.48 (m, 5H, A,  $H_2+H_3+H_5+H_6$ , B,  $H_{11}$ ), 7.41 (t, 1H, B,  $J_{4-3} = J_{4-5} = 7.4$  Hz,  $H_4$ ), 7.24 (t, 2H, B,  $J_{3-2} = J_{3-4} = J_{10-9} = J_{10-11} = 5.9$  Hz,  $H_3+H_{10}$ ).  $^{13}\text{C}$  NMR (100 MHz, DMSO- $d_6$ )  $\delta$ : 169.20 (COOH), 167.55 (C=O), 141.41 (A,  $C_4$ ), 140.79 + 140.76 (B,  $C_6+C_7$ ), 136.14 (B,  $C_8$ ), 135.19 (A,  $C_2+C_6$ ), 131.67 (B,  $C_1$ ), 131.42 + 131.07 + 130.45 + 130.11 + 129.84 (B,  $C_2+C_3+C_4+C_9+C_{11}$ ), 127.88 + 127.78 + 127.55 (B,  $C_5+C_{10}+C_{12}$ ), 121.06 (A,  $C_3+C_5$ ), 117.14 (A,  $C_1$ ), 105.89 (CN). MS [ $m/z$  (% abundance)]: 152 (70), 181 (100), 225 (30), 422 (10). Elemental analysis calculated (%) for  $\text{C}_{21}\text{H}_{14}\text{N}_2\text{O}_3\text{Se} \cdot 2\text{H}_2\text{O}$ : C: 55.15, H: 3.97, N: 6.13; found: C: 55.39, H: 3.59, N: 6.22.

**4.1.4.7. 2-[(4-Selenocyanatophenyl)carbamoyl]cyclohexanecarboxylic acid (7b).** From cis-1,2-cyclohexanecarboxylic anhydride. Conditions: 24 h at room temperature. The product was kept under stirring with water (25 mL) for 2 h, filtered and then washed with ethyl ether (2  $\times$  25 mL). A white powder was obtained. Yield: 47.0%. Mp: 150–151 °C. IR (KBr)  $\text{cm}^{-1}$ : 3335 (NH), 2152 (CN), 1702 (C=O, carboxylic acid), 1677 (C=O, amide).  $^1\text{H}$  NMR (400 MHz, DMSO- $d_6$ )  $\delta$ : 11.99 (bs, 1H, COOH), 9.95 (s, 1H, NH), 7.66 (d, 2H, A,  $J_{2-3} = J_{6-5} = 8.5$  Hz,  $H_2+H_6$ ), 7.62 (d, 2H, A,  $J_{3-2} = J_{5-6} = 8.5$  Hz,  $H_3+H_5$ ), 2.94 (d, 1H, B,  $J_{1-\text{Hchex}} = 4.0$  Hz,  $H_1$ ), 2.60 (d, 1H, B,  $J_{\text{chex}-1} = 4.0$  Hz,  $H_{\text{chex}}$ ), 2.09 (d, 1H, B,  $J = 9.7$  Hz,  $H_{\text{chex}}$ ), 1.99 (d, 1H, B,  $J = 8.8$  Hz,  $H_{\text{chex}}$ ), 1.82–1.57 (m, 3H, B,  $3\text{Hchex}$ ), 1.48–1.24 (m, 3H, B,  $3\text{Hchex}$ ).  $^{13}\text{C}$  NMR (100 MHz, DMSO- $d_6$ )  $\delta$ : 175.55 (COOH), 173.56 (C=O), 141.39 (A,  $C_4$ ), 135.24 (A,  $C_2+C_6$ ), 120.76 (A,  $C_3+C_5$ ), 116.18 (A,  $C_1$ ), 105.87 (CN), 43.05 + 42.42 (B,  $C_1+C_2$ ), 28.06 + 25.64 + 24.44 + 22.78 (B,  $C_3+C_4+C_5+C_6$ ). MS [ $m/z$  (% abundance)]: 67 (90), 81 (93), 118 (100), 198 (60), 334 (100). Elemental analysis calculated (%) for  $\text{C}_{15}\text{H}_{16}\text{N}_2\text{O}_3\text{Se} \cdot \text{H}_2\text{O}$ : C: 48.79, H: 4.91, N: 7.59; found: C: 48.56, H: 4.72, N: 7.66.

**4.1.4.8. 3-[(4-Selenocyanatophenyl)carbamoyl]-7-oxabicyclo[2.2.1]hept-5-ene-2-carboxylic acid (8b).** From 3,6-epoxy-1,2,3,6-tetrahydrophthalic anhydride obtained by the classic procedure described for a Diels-Alder reaction using furan and maleic anhydride as reagents to yield the Diels-Alder adduct. Conditions: 24 h at room temperature. The product was kept under stirring with water (25 mL) for 4 h, filtered and then washed with ethyl ether (2  $\times$  25 mL). A light-yellow powder was obtained. Yield: 20.3%. Mp: 155–156 °C. IR (KBr)  $\text{cm}^{-1}$ : 3267 (NH), 1711 (C=O carboxylic acid), 1689 (C=O, amide).  $^1\text{H}$  NMR (400 MHz, DMSO- $d_6$ )  $\delta$ : 12.19 (s, 1H, COOH), 10.03 (s, 1H, NH), 7.65 (d, 2H, A,  $J_{2-3} = J_{6-5} = 9.0$  Hz,  $H_2+H_6$ ), 7.62 (d, 2H, A,  $J_{3-2} = J_{5-6} = 9.0$  Hz,  $H_3+H_5$ ), 6.50 (s, 2H, B,  $H_3+H_5$ ), 5.14 (s, 1H, B,  $H_5$ ), 5.06 (s, 1H, B,  $H_2$ ), 2.82 (d, 1H, B,  $J_{1-6} = 9.1$  Hz,  $H_1$ ), 2.71 (d, 1H, B,  $J_{6-1} = 9.1$  Hz,  $H_6$ ).  $^{13}\text{C}$  NMR (100 MHz, DMSO- $d_6$ )  $\delta$ : 173.08 (COOH), 170.48 (C=O), 141.07 (A,  $C_4$ ), 137.49 + 137.08 (B,  $C_4+C_5$ ), 135.29 (A,  $C_2+C_6$ ), 120.79 (A,  $C_3+C_5$ ),

116.51 (A,  $C_1$ ), 105.93 (CN), 80.82 + 79.61 (B,  $C_3+C_6$ ), 47.96 + 47.36 (B,  $C_1+C_2$ ).  $^{77}\text{Se}$  NMR (76 MHz, DMSO- $d_6$ )  $\delta$ : 320.95 (SeCN). MS [ $m/z$  (% abundance)]: 68 (100), 118 (100), 198 (25), 278 (10). Elemental analysis calculated (%) for  $\text{C}_{15}\text{H}_{12}\text{N}_2\text{O}_4\text{Se} \cdot \frac{1}{2}\text{H}_2\text{O}$ : C: 48.35, H: 3.49, N: 7.52; found: C: 48.30, H: 3.70, N: 7.53.

## 4.2. Biological evaluation

### 4.2.1. Cell cultures

Cell lines were purchased from the American Type Culture Collection (ATCC). PC-3, HTB-54, HT-29, MOLT-4, CCRF-CEM, K-562 and MCF-7 cell lines were grown in RPMI 1640 medium (Gibco) supplemented with 10% fetal bovine serum (FBS; Gibco), 100 units/mL penicillin and 100 mg/mL streptomycin (Gibco). BEAS-2B cell line (normal epithelial lung) was cultured in DMEM (Gibco), 10% FBS, 100 units/mL penicillin and 100  $\mu\text{g}/\text{mL}$  streptomycin. 184B5 cells were grown in DMEM/F12 medium supplemented with 5% FBS, 1  $\times$  ITS (Lonza), 100 nM hydrocortisone (Aldrich), 2 mM sodium pyruvate (Lonza), 20 ng/mL EGF (Sigma-Aldrich), 0.3 nM *trans*-retinoic acid (Sigma-Aldrich), 100 units/mL penicillin and 100 mg/mL streptomycin. Cells were maintained at 37 °C and 5%  $\text{CO}_2$ .

### 4.2.2. Cytotoxic and antiproliferative activities

Cell viability was determined using the MTT 3-(4,5-dimethylthiazol-2-yl)-2,5-diphenyl-tetrazolium bromide) method at 10 and 100  $\mu\text{M}$  to perform the screening. In order to build full dose-response curves five different doses ranging from 0.01 to 100  $\mu\text{M}$ , for some compounds lower doses were needed in order to reach 50% cell growth. Depending on cell size, 8,000 to 40,000 cells were seeded per well in 96-well plates and incubated overnight. Then treated with the compounds for 48 h, cells were then incubated with 50  $\mu\text{L}$  of MTT (2 mg/mL stock) for 4 h, medium was removed by aspiration and formazan crystals dissolved in 150  $\mu\text{L}$  of DMSO. The absorbance was measured at 550 nm in a microplate reader (Sunrise reader, Tecan). At least three independent experiments performed in quadruplicate were analysed. Results are expressed as  $\text{GI}_{50}$ , the concentration that reduces by 50% the growth of treated cells with respect to untreated controls, TGI, the concentration that completely inhibits cell growth, and  $\text{LC}_{50}$ , the concentration that kills 50% of the cells.

### 4.2.3. Evaluation of cell cycle progression and cell death

A fixed population of MCF-7 cells per flask were seeded in 25  $\text{cm}^2$  flasks then incubated overnight. Cultures were treated with the corresponding amount of compounds **10a**, **8b**, DMSO (control) or 6  $\mu\text{M}$  camptothecin (positive control). Seeded population was dependent on studied time point: 3  $\times 10^6$  cells/flask for 24 h or shorter treatment, 2  $\times 10^6$  cells/flasks for 48 h treatment and finally 1  $\times 10^6$  cells/flask for 72 h experiments. Apo-Direct kit (BD Pharmingen) was used to determine cell cycle distribution and cell death percentage. Cells were fixed in a 1% paraformaldehyde solution in PBS for 30–40 min at 0 °C, washed with PBS twice and incubated for 30 min with 70% ethanol on ice. Staining was performed following manufacturer's protocol and samples were analysed by flow cytometry using a Counter Epics XL cytometer (Beckman Counter).

Inhibition assays cells were pre-treated with 50  $\mu\text{M}$  of the pan-caspase inhibitor Z-VAD-FMK (BD Pharmingen) or 100 nM of the autophagy inhibitor wortmannin (Santa Cruz) for 1 h or 10  $\mu\text{M}$  of chloroquine (Sigma Aldrich). The cells were treated with 80  $\mu\text{M}$  of **8b** or **10a**, DMSO was added to the control cells. Samples were processed following the same methodology stated above. At least three independent experiments were performed in duplicate.

#### 4.2.4. Statistical analysis

Statistical data represent the mean  $\pm$  SEM of at least three independent experiments performed in duplicate. Mann-Whitney *U* test was used to establish statistical significance of differences between control and treatment groups. GraphPad Prism version 7 was used, significant differences were considered at  $p < 0.05$ .

#### 4.2.5. Protein analysis

Proteins were detected by western blot. Specific antibodies for LC3B, Beclin-1 (D40C5), SQSTM1/p62, AMPK, JNK, pAKT (S473) and the PI3K catalytic subunit p110 $\alpha$  were obtained from Cell Signalling. Anti-actin (H-300) was from Santa Cruz Biotechnology. Anti-rabbit IgG conjugated with peroxidase (Cell Signaling) was used as secondary antibody.

#### Acknowledgments

The research leading to these results has received funding from “la Caixa” Banking Foundation. P. Garnica wishes to express his gratitude to the Asociación de Amigos de la Universidad de Navarra for the pre-doctoral fellowship. Furthermore, the authors wish to express their gratitude to the Plan de Investigación de la Universidad de Navarra, PIUNA (Ref 2014–26) as well as Calgary Foundation for financial support for the project.

#### Appendix A. Supplementary data

Supplementary data to this article can be found online at <https://doi.org/10.1016/j.ejmech.2019.04.074>.

#### References

- [1] R.L. Siegel, K.D. Miller, A. Jemal, Cancer statistics, 2018, *Ca-Cancer, J. Clin. Oncol.* 36 (2018) 7–30. <https://doi.org/10.3322/caac.21442>.
- [2] P. Bhat, J. Kriel, B. Shubha Priya, Basappa, N.S. Shivananju, B. Loos, Modulating autophagy in cancer therapy: advancements and challenges for cancer cell death sensitization, *Biochem. Pharmacol.* 147 (2018) 170–182. <https://doi.org/10.1016/j.bcp.2017.11.021>.
- [3] C. Bi, N. Zhang, P. Yang, C. Ye, Y. Wang, T. Fan, R. Shao, H. Deng, D. Song, Synthesis, biological evaluation, and autophagy mechanism of 12N-substituted sophoridinamines as novel anticancer agents, *ACS Med. Chem. Lett.* 8 (2017) 245–250. <https://doi.org/10.1021/acsmedchemlett.6b00466>.
- [4] Y.Y. Zhou, Y. Li, W.Q. Jiang, L.F. Zhou, MAPK/JNK signalling: a potential autophagy regulation pathway, *Biosci. Rep.* 35 (2015). <https://doi.org/10.1042/BSR20140141>.
- [5] D.D. Li, L.L. Wang, R. Deng, J. Tang, Y. Shen, J.F. Guo, Y. Wang, L.P. Xia, et al., The pivotal role of c-JUN NH2-terminal kinase-mediated Beclin 1 expression during anticancer agents-induced autophagy in cancer cells, *Oncogene* 28 (2009) 886–898. <https://doi.org/10.1038/onc.2008.441>.
- [6] R.C. Russell, H.X. Yuan, K.L. Guan, Autophagy regulation by nutrient signaling, *Cell Res.* 24 (2014) 42–57. <https://doi.org/10.1038/cr.2013.166>.
- [7] K. Inoki, T. Zhu, K.L. Guan, TSC2 mediates cellular energy response to control cell growth and survival, *Cell* 115 (2003) 577–590. [https://doi.org/10.1016/S0092-8674\(03\)00929-2](https://doi.org/10.1016/S0092-8674(03)00929-2).
- [8] S. Kanno, S. Yomogida, A. Tomizawa, H. Yamazaki, K. Ukai, R.E.P. Mangindaan, M. Namikoshi, M. Ishikawa, Papuamine causes autophagy following the reduction of cell survival through mitochondrial damage and JNK activation in MCF-7 human breast cancer cells, *Int. J. Oncol.* 43 (2013) 1413–1419. <https://doi.org/10.3892/ijo.2013.2093>.
- [9] Z.L. Sun, J.L. Dong, J. Wu, Juglanin induces apoptosis and autophagy in human breast cancer progression via ROS/JNK promotion, *Biomed. Pharmacother.* 85 (2017) 303–312. <https://doi.org/10.1016/j.biopha.2016.11.030>.
- [10] S. Kang, J.E. Kim, N.R. Song, S.K. Jung, M.H. Lee, J.S. Park, M.H. Yeom, A.M. Bode, Z. Dong, K.W. Lee, The ginsenoside 20-o-beta-d-glucopyranosyl-20(S)-protopanaxadiol induces autophagy and apoptosis in human melanoma via AMPK/JNK phosphorylation, *PLoS One* 9 (2014) e104305. <https://doi.org/10.1371/journal.pone.0104305>.
- [11] A. Puissant, G. Robert, N. Fenouille, F. Luciano, J.P. Cassuto, S. Raynaud, P. Auberger, Resveratrol promotes autophagic cell death in chronic myelogenous leukemia cells via JNK-mediated p62/SQSTM1 expression and ampk activation, *Cancer Res.* 70 (2010) 1042–1052. <https://doi.org/10.1158/0008-5472.CAN-09-3537>.
- [12] Q. Miao, J. Xu, A. Lin, X. Wu, L. Wu, W. Xie, Recent advances for the synthesis of selenium-containing small molecules as potent antitumor agents, *Curr. Med. Chem.* 25 (2017) 2009–2033. <https://doi.org/10.2174/0929867325666171129220544>.
- [13] D. Bartolini, L. Sancineto, A. Fabro de Bem, K.D. Tew, C. Santi, R. Radi, P. Toquato, F. Galli, Selenocompounds in cancer therapy: an overview, *Adv. Cancer Res.* 136 (2017) 259–302. <https://doi.org/10.1016/bs.acr.2017.07.007>.
- [14] Y. Yang, H. Luo, K. Hui, Y. Ci, K. Shi, G. Chen, L. Shi, C. Xu, Selenite-induced autophagy antagonizes apoptosis in colorectal cancer cells *in vitro* and *in vivo*, *Oncol. Rep.* 35 (2016) 1255–1264. <https://doi.org/10.3892/or.2015.4484>.
- [15] J.C. Wu, F.Z. Wang, M.L. Tsai, C.Y. Lo, V. Badmaev, C.T. Ho, Y.J. Wang, M.H. Pan, Se-allylselenocysteine induces autophagy by modulating the AMPK/mTOR signaling pathway and epigenetic regulation of PCDH17 in human colorectal adenocarcinoma cells, *Mol. Nutr. Food Res.* 59 (2015) 2511–2522. <https://doi.org/10.1002/mnfr.201500373>.
- [16] Y.F. Zou, P.Y. Niu, J. Yang, J. Yuan, T.C. Wu, X.M. Chen, The JNK signaling pathway is involved in sodium-selenite-induced apoptosis mediated by reactive oxygen in HEPG2 cells, *Cancer Biol. Ther.* 7 (2008) 689–696. <https://doi.org/10.4161/cbt.7.5.5688>.
- [17] K. Wang, X.T. Fu, Y. Li, Y.J. Hou, M.F. Yang, J.Y. Sun, S.Y. Yi, C.D. Fan, et al., Induction of S-phase arrest in human glioma cells by selenocysteine, a natural selenium-containing agent via triggering reactive oxygen species-mediated DNA damage and modulating MAPKs and AKT pathways, *Neurochem. Res.* 41 (2016) 1439–1447. <https://doi.org/10.1007/s11064-016-1854-8>.
- [18] P. Chakraborty, S.S. Roy, A. Basu, S. Bhattacharya, Sensitization of cancer cells to cyclophosphamide therapy by an organoselenium compound through ROS-mediated apoptosis, *Biomed. Pharmacother.* 84 (2016) 1992–1999. <https://doi.org/10.1016/j.biopha.2016.11.006>.
- [19] C. Kim, J. Lee, M.-S. Park, Synthesis of new diorganodiselenides from organic halides: their antiproliferative effects against human breast cancer MCF-7 cells, *Arch. Pharm. Res. (Seoul)* 38 (2014) 659–665. <https://doi.org/10.1007/s12272-014-0407-4>.
- [20] D. Plano, Y. Baquedano, E. Ibanez, I. Jimenez, J.A. Palop, J.E. Spallholz, C. Sanmartin, Antioxidant-prooxidant properties of a new organoselenium compound library, *Molecules* 15 (2010) 7292–7312. <https://doi.org/10.3390/molecules15107292>.
- [21] P. Garnica, I. Encio, D. Plano, J.A. Palop, C. Sanmartin, Combined acylselenourea-diselenide structures: new potent and selective antitumoral agents as autophagy activators, *ACS Med. Chem. Lett.* 9 (2018) 306–311. <https://doi.org/10.1021/acsmedchemlett.7b00482>.
- [22] V. Bala, S. Rao, P. Li, S. Wang, C.A. Prestidge, Lipophilic prodrugs of SN38: synthesis and *in vitro* characterization toward oral chemotherapy, *Mol. Pharm.* 13 (2015) 287–294. <https://doi.org/10.1021/acs.molpharmaceut.5b00785>.
- [23] M. Majekova, J. Ballekova, M. Prnova, M. Stefek, Structure optimization of tetrahydropyridindole-based aldose reductase inhibitors improved their efficacy and selectivity, *Bioorg. Med. Chem.* 25 (2017) 6353–6360. <https://doi.org/10.1016/j.bmc.2017.10.005>.
- [24] G. Huang, A. Drakopoulos, M. Saedtler, H. Zou, L. Meinel, J. Heilmann, M. Decker, Cytotoxic properties of the alkaloid rutaecarpine and its oligocyclic derivatives and chemical modifications to enhance water-solubility, *Bioorg. Med. Chem. Lett.* 27 (2017) 4937–4941. <https://doi.org/10.1016/j.bmcl.2017.08.045>.
- [25] V. Gota, J.S. Goda, K. Doshi, A. Patil, S. Sunderajan, K. Kumar, M. Varne, A. Kunwar, V.K. Jain, I. Priyadarshini, Biodistribution and pharmacokinetic study of 3,3'-diseleno dipropionic acid (DSEPA), a synthetic radioprotector, in mice, *Eur. J. Drug Metabol.* 41 (2015) 839–844. <https://doi.org/10.1007/s13318-015-0301-6>.
- [26] K.E. Machado, K.N. Oliveira, L. Santos-Bubniak, M.A. Licinio, R.J. Nunes, M.C. Santos-Silva, Evaluation of apoptotic effect of cyclic imide derivatives on murine B16F10 melanoma cells, *Bioorg. Med. Chem.* 19 (2011) 6285–6291. <https://doi.org/10.1016/j.bmc.2011.09.008>.
- [27] D. Rosolen, I.F. Kretzer, E. Winter, V.F. Noldin, I.A. Rodrigues do Carmo, F.B. Filippin-Monteiro, V. Cechinel-Filho, T.B. Creczynski-Pasa, N-phenylmaleimides affect adipogenesis and present antitumor activity through reduction of FASN expression, *Chem. Biol. Interact.* 258 (2016) 10–20. <https://doi.org/10.1016/j.cbi.2016.08.005>.
- [28] B. Romano, D. Plano, I. Encio, J.A. Palop, C. Sanmartin, *In vitro* radical scavenging and cytotoxic activities of novel hybrid selenocarbamates, *Bioorg. Med. Chem.* 23 (2015) 1716–1727. <https://doi.org/10.1016/j.bmc.2015.02.048>.
- [29] E. Dominguez-Alvarez, D. Plano, M. Font, A. Calvo, C. Prior, C. Jacob, J.A. Palop, C. Sanmartin, Synthesis and antiproliferative activity of novel selenoester derivatives, *Eur. J. Med. Chem.* 73 (2014) 153–166. <https://doi.org/10.1016/j.ejmech.2013.11.034>.
- [30] V. Alcolea, D. Plano, D.N. Karelia, J.A. Palop, S. Amin, C. Sanmartin, A.K. Sharma, Novel seleno- and thio-urea derivatives with potent *in vitro* activities against several cancer cell lines, *Eur. J. Med. Chem.* 113 (2016) 134–144. <https://doi.org/10.1016/j.ejmech.2016.02.042>.
- [31] V. Alcolea, D. Plano, I. Encio, J.A. Palop, A.K. Sharma, C. Sanmartin, Chalcogen containing heterocyclic scaffolds: new hybrids with antitumoral activity, *Eur. J. Med. Chem.* 123 (2016) 407–418. <https://doi.org/10.1016/j.ejmech.2016.07.042>.
- [32] N. Diaz-Argelich, I. Encio, D. Plano, A.P. Fernandes, J.A. Palop, C. Sanmartin, Novel methylselenoesters as antiproliferative agents, *Molecules* 22 (2017) 1288. <https://doi.org/10.3390/molecules22081288>.
- [33] M. Diaz, R. Gonzalez, D. Plano, J.A. Palop, C. Sanmartin, I. Encio, A diphenyldiselenide derivative induces autophagy via JNK in HTB-54 lung

- cancer cells, *J. Cell Mol. Med.* 22 (2018) 289–301. <https://doi.org/10.1111/jcmm.13318>.
- [34] Z. Han, B. Li, J. Wang, X. Zhang, Z. Li, L. Dai, M. Cao, J. Jiang, Norcantharidin inhibits SK-N-SH neuroblastoma cell growth by induction of autophagy and apoptosis, *Technol. Canc. Res. Treat.* 16 (2016) 33–44. <https://doi.org/10.1177/1533034615624583>.
- [35] M. Dalvai, K. Bystricky, Cell cycle and anti-estrogen effects synergize to regulate cell proliferation and ER target gene expression, *PLoS One* 5 (2010) e11011. <https://doi.org/10.1371/journal.pone.0011011>.
- [36] H. Hamouchene, V.M. Arlt, I. Giddings, D.H. Phillips, Influence of cell cycle on responses of MCF-7 cells to benzo[a]pyrene, *BMC Genomics* 12 (2011) 333. <https://doi.org/10.1186/1471-2164-12-333>.
- [37] M. Hamada, H. Kameyama, S. Iwai, Y. Yura, Induction of autophagy by sphingosine kinase 1 inhibitor PF-543 in head and neck squamous cell carcinoma cells, *Cell Death Dis.* 3 (2017) 17047. <https://doi.org/10.1038/cddiscovery.2017.47>.
- [38] P. Fabbriozio, S. Amadio, S. Apolloni, C. Volonte, P2x7 receptor activation modulates autophagy in SOD1-G93A mouse microglia, *Front. Cell. Neurosci.* 11 (2017) 249. <https://doi.org/10.3389/fncel.2017.00249>.
- [39] H.J. Jung, J.H. Kang, S. Choi, Y.K. Son, K.R. Lee, J.K. Seong, S.Y. Kim, S.H. Oh, Phorbis nil (PN) induces apoptosis and autophagy in lung cancer cells and autophagy inhibition enhances PN-induced apoptosis, *J. Ethnopharmacol.* 208 (2017) 253–263. <https://doi.org/10.1016/j.jep.2017.07.020>.
- [40] D.J. Klionsky, K. Abdelmohsen, A. Abe, M.J. Abedin, H. Abeliovich, A. Acevedo Arozena, H. Adachi, C.M. Adams, et al., Guidelines for the use and interpretation of assays for monitoring autophagy, *Autophagy* 12 (2016) 1–222. <https://doi.org/10.1080/15548627.2015.1100356>. third ed.
- [41] K. Wang, C. Zhang, J. Bao, X. Jia, Y. Liang, X. Wang, M. Chen, H. Su, et al., Synergistic chemopreventive effects of curcumin and berberine on human breast cancer cells through induction of apoptosis and autophagic cell death, *Sci. Rep.* 6 (2016) 26064. <https://doi.org/10.1038/srep26064>.
- [42] S. Faes, O. Dormond, PI3K and AKT: unfaithful partners in cancer, *Int. J. Mol. Sci.* 16 (2015) 21138–21152. <https://doi.org/10.3390/ijms160921138>.
- [43] X. Wu, S. Renuse, N.A. Sahasrabudhe, M.S. Zahari, R. Chaerkady, M.S. Kim, R.S. Nirujogi, M. Mohseni, et al., Activation of diverse signalling pathways by oncogenic PIK3CA mutations, *Nat. Commun.* 5 (2014) 4961. <https://doi.org/10.1038/ncomms5961>.
- [44] A. Guerrero-Zotano, I.A. Mayer, C.L. Arteaga, PI3K/AKT/mTOR: role in breast cancer progression, drug resistance, and treatment, *Cancer Metastasis Rev.* 35 (2016) 515–524. <https://doi.org/10.1007/s10555-016-9637-x>.
- [45] X.L. Xu, J. Sun, R.L. Song, M.E. Doscas, A.J. Williamson, J.S. Zhou, J. Sun, X.N. Jiao, X.F. Liu, Y. Li, Inhibition of p70 S6 kinase (S6K1) activity by A77 1726, the active metabolite of leflunomide, induces autophagy through TAK1-mediated AMPK and JNK activation, *Oncotarget* 8 (2017) 30438–30454. <https://doi.org/10.18632/oncotarget.16737>.
- [46] J.N. Hutchinson, J. Jin, R.D. Cardiff, J.R. Woodgett, W.J. Muller, Activation of AKT-1 (PKB-alpha) can accelerate ERBB-2-mediated mammary tumorigenesis but suppresses tumor invasion, *Cancer Res.* 64 (2004) 3171–3178. <https://doi.org/10.1158/0008-5472>.
- [47] S. Brolih, S.K. Parks, V. Vial, J. Durivault, L. Mostosi, J. Pouyssegur, G. Pages, V. Picco, AKT1 restricts the invasive capacity of head and neck carcinoma cells harboring a constitutively active PI3 kinase activity, *BMC Canc.* 18 (2018) 249. <https://doi.org/10.1186/s12885-018-4169-0>.